Long-baseline Oscillations

Stefan Söldner-Rembold
University of Manchester

DUNE-UK Meeting
3 July 2022

Pontecorvo–Maki–Nakagawa–Sakata Matrix

$$\begin{pmatrix} \nu_e \\ \nu_\mu \\ \nu_\tau \end{pmatrix} = U_{\mathrm{PMNS}} \begin{pmatrix} \nu_1 \\ \nu_2 \\ \nu_3 \end{pmatrix}$$

$$U_{\mathrm{PMNS}} = \begin{pmatrix} c_{12} & s_{12} & 0 \\ -s_{12} & c_{12} & 0 \\ 0 & 0 & 1 \end{pmatrix} \begin{pmatrix} c_{13} & 0 & s_{13}e^{-i\delta} \\ 0 & 1 & 0 \\ -s_{13}e^{i\delta} & 0 & c_{13} \end{pmatrix} \begin{pmatrix} 1 & 0 & 0 \\ 0 & c_{23} & s_{23} \\ 0 & -s_{23} & c_{23} \end{pmatrix}$$

$$c_{ij} = \cos\theta_{ij}; s_{ij} = \sin\theta_{ij}$$

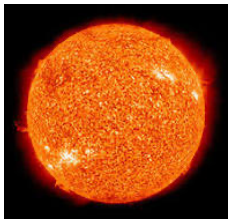

- θ_{12}: “solar mixing angle”
- mixes ν_e with ν_1 and ν_2

θ_{13}: mixes ν_e with ν_3

δ: complex phase

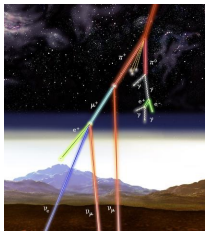

- θ_{23}: “atmospheric mixing angle”
- mixes ν_μ with ν_τ

Pontecorvo–Maki–Nakagawa–Sakata Matrix

solar “reactor” atmospheric

$$U_{\mathrm{PMNS}} = \begin{pmatrix} c_{12} & s_{12} & 0 \\ -s_{12} & c_{12} & 0 \\ 0 & 0 & 1 \end{pmatrix} \begin{pmatrix} c_{13} & 0 & s_{13}e^{-i\delta} \\ 0 & 1 & 0 \\ -s_{13}e^{i\delta} & 0 & c_{13} \end{pmatrix} \begin{pmatrix} 1 & 0 & 0 \\ 0 & c_{23} & s_{23} \\ 0 & -s_{23} & c_{23} \end{pmatrix}$$

$$c_{ij} = \cos\theta_{ij}; s_{ij} = \sin\theta_{ij}$$

$$\theta_{12} = 33.44^{\circ}{}^{+0.78^{\circ}}_{-0.75^{\circ}}$$

$$\theta_{23} = 49.0^{\circ}{}^{+1.1^{\circ}}_{-1.4^{\circ}}$$

- “Small” angle θ_{13} mixes ν_e with ν_3
- Look for ν_e mixing driven by Δm^2_{32}
- Reactor: anti-ν_e disappearance
- Accelerator: ν_e appearance in ν_μ beam

→ sensitive to θ_{13} and δ (and MO).

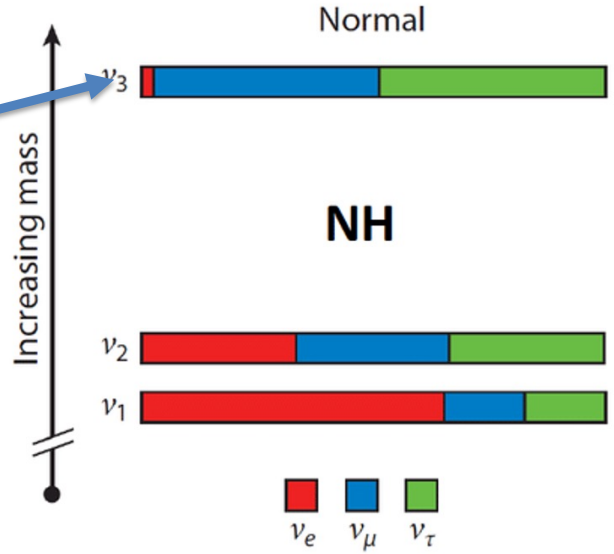

$$\Delta m^2_{32} = 2.4 \times 10^{-3}\,\mathrm{eV}^2$$

$$\Delta m^2_{21} = 7.8 \times 10^{-5}\,\mathrm{eV}^2$$

The PMNS Matrix and CP violation

complex CP phase

$$U_{\mathrm{PMNS}} = \begin{pmatrix} U_{e1} & U_{e2} & U_{e3} \\ U_{\mu 1} & U_{\mu 2} & U_{\mu 3} \\ U_{\tau 1} & U_{\tau 2} & U_{\tau 3} \end{pmatrix} = \begin{pmatrix} 1 & 0 & 0 \\ 0 & c_{23} & s_{23} \\ 0 & -s_{23} & c_{23} \end{pmatrix} \begin{pmatrix} c_{13} & 0 & s_{13}e^{-i\delta} \\ 0 & 1 & 0 \\ -s_{13}e^{i\delta} & 0 & c_{13} \end{pmatrix} \begin{pmatrix} c_{12} & s_{12} & 0 \\ -s_{12} & c_{12} & 0 \\ 0 & 0 & 1 \end{pmatrix}$$

$$s_{ij} = \sin\theta_{ij} \; ; \; c_{ij} = \cos\theta_{ij}$$

$$\delta \neq \{0, \pi\}$$

CP Violation involving neutrinos might provide support for *Leptogenesis* as mechanism to generate the Universe's matter-antimatter asymmetry.

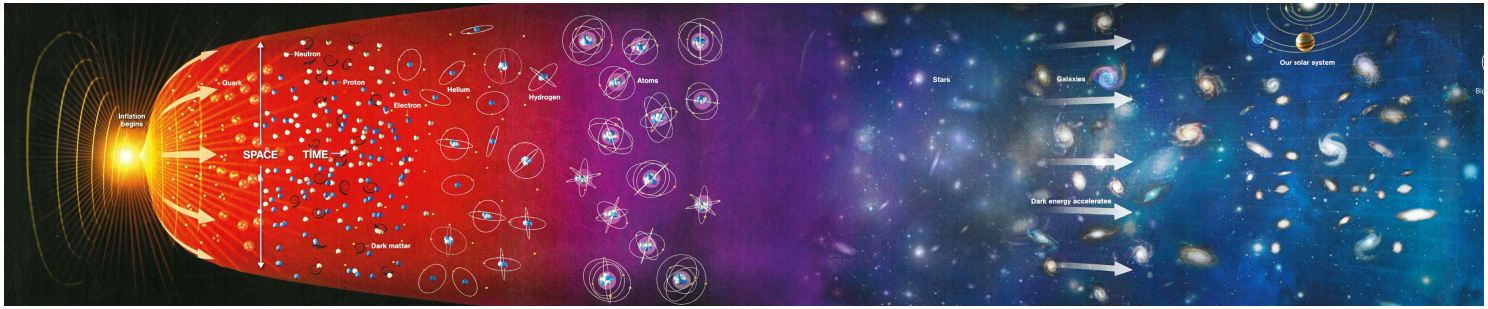

Neutrino flavour oscillations

$$P(\nu_\alpha \to \nu_\beta) = \sin^2(2\theta)\sin^2\left(1.27\frac{\Delta m^2_{21}[\mathrm{eV}^2]L[\mathrm{km}]}{E[\mathrm{GeV}]}\right)$$

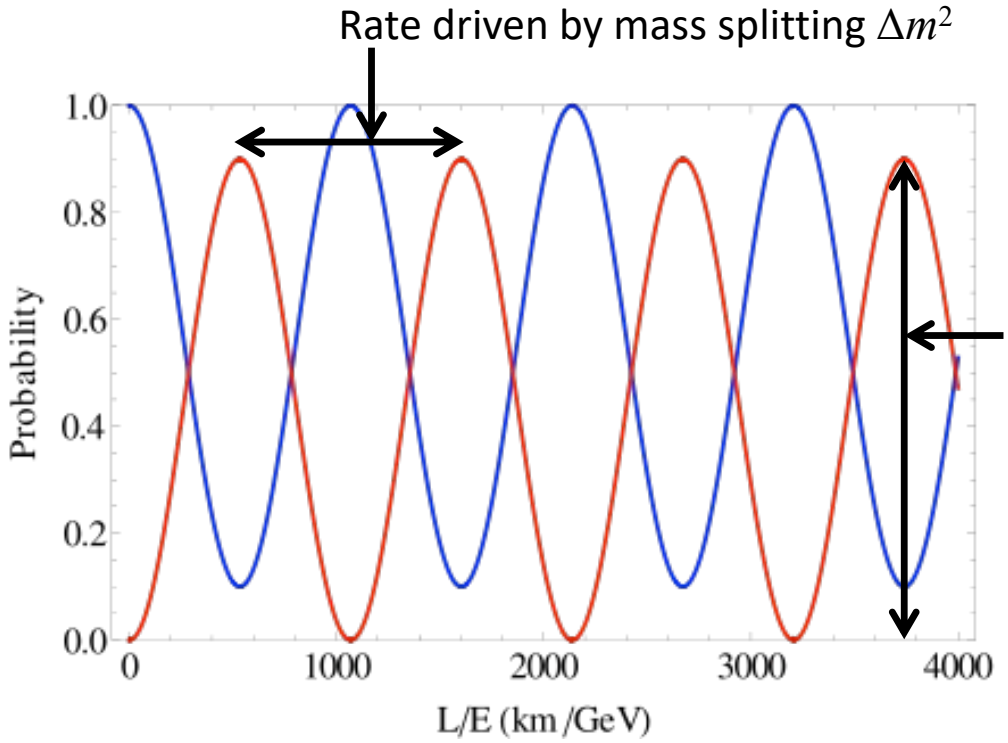

ν_α component

ν_β component

Amplitude driven by mixing angle $\sin^2(2\theta)$

Baseline, energy, and frequency

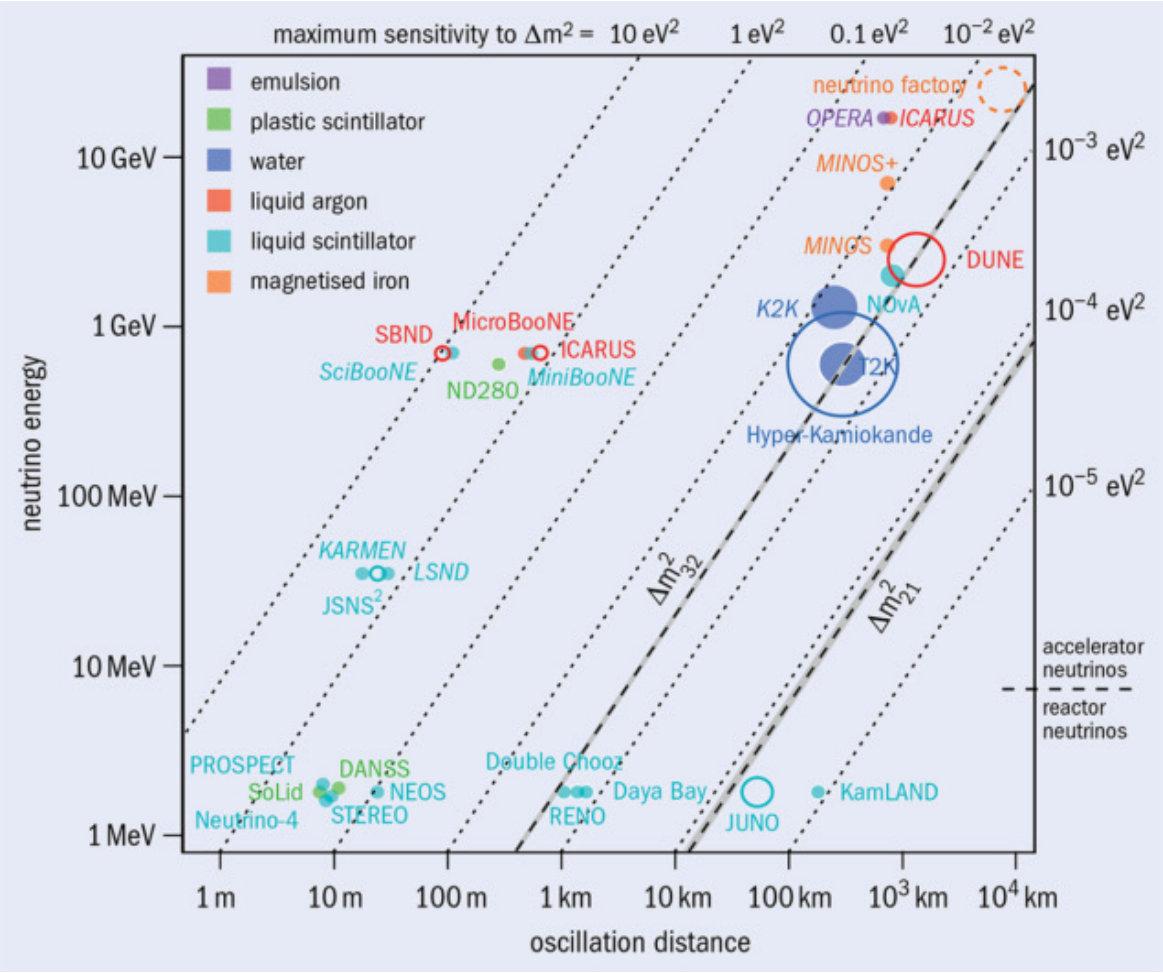

CERN Courier, 2020

$$\frac{\Delta m^2 L}{4E}$$

Optimizing detectors for neutrino oscillations

L/E(1st max) = 500 km/GeV
L/E (2nd max) = 1700 km/GeV

L ≈ 300 km

- no matter effects.
- use narrow width neutrino beam (off axis) with E < 1 GeV
- observe first oscillation maximum
- "counting experiment"

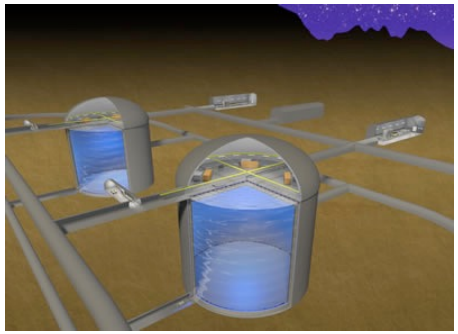

Water Cherenkov (HK)

L = 1300 km

- matter effects
- use broad-band neutrino beam (on axis).
- observe first and second oscillation maximum.
- unfold CP and MO effects through energy dependence

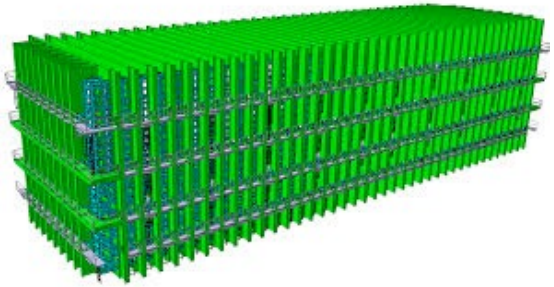

Liquid argon (DUNE)

Off-axis vs on-axis beams

T2K at 2.5 degrees

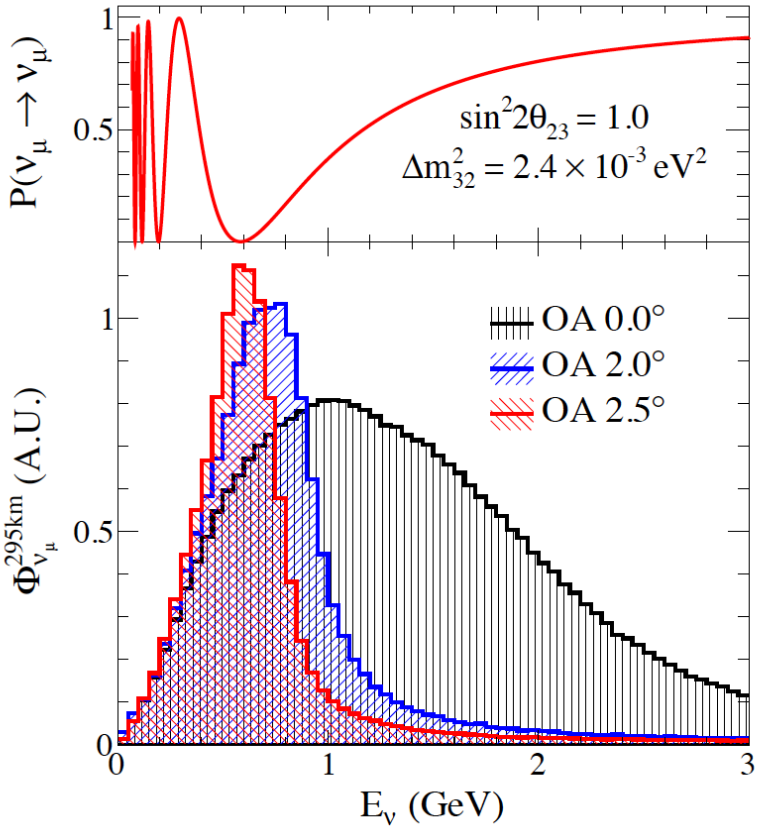

DUNE on-axis beam

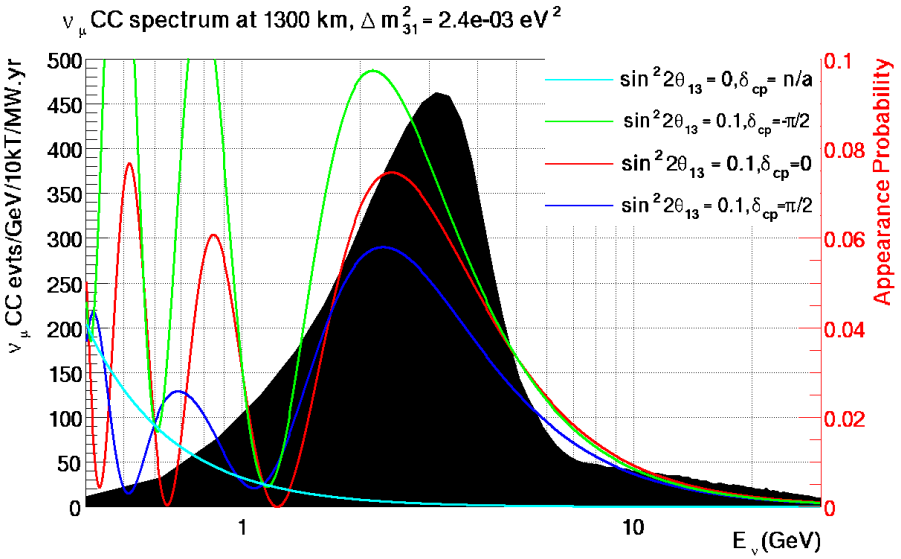

ν_e appearance gives access to δ

$$P(\nu_\mu \to \nu_e) \approx \sin^2\theta_{23}\,\sin^2 2\theta_{13}\,\frac{\sin^2(\Delta_{31}-aL)}{(\Delta_{31}-aL)^2}\Delta_{31}^2$$
$$+\sin 2\theta_{23}\,\sin 2\theta_{13}\,\sin 2\theta_{12}\,\frac{\sin(\Delta_{31}-aL)}{(\Delta_{31}-aL)}\Delta_{31}\,\frac{\sin(aL)}{aL}\Delta_{21}\cos(\Delta_{31}-\delta)$$
$$+\cos^2\theta_{23}\sin^2 2\theta_{12}\,\frac{\sin(aL)}{aL}\Delta_{21}^2$$

$$a = \frac{G_F N_e}{\sqrt{2}} \qquad \Delta_{ij} = \frac{\Delta m_{ij}^2 L}{4E}$$

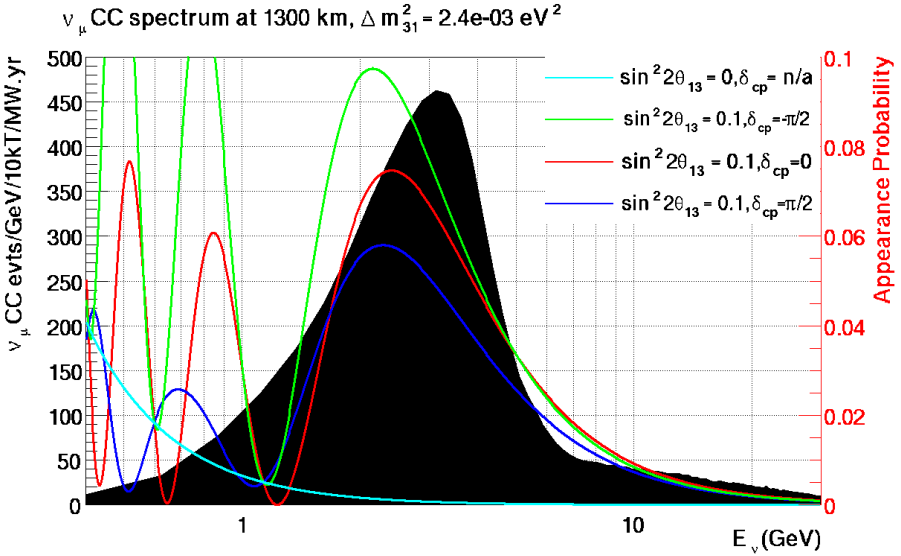

- ν_e appearance amplitude depends simultaneously on θ_{13}, θ_{23}, δ_{CP}, and matter effects –
- Measurements of all four possible in a single experiment.

ν_e appearance gives access to δ

$$P(\nu_\mu \to \nu_e) \approx \sin^2\theta_{23}\sin^2 2\theta_{13}\frac{\sin^2(\Delta_{31}-aL)}{(\Delta_{31}-aL)^2}\Delta_{31}^2$$
$$+\sin 2\theta_{23}\sin 2\theta_{13}\sin 2\theta_{12}\frac{\sin(\Delta_{31}-aL)}{(\Delta_{31}-aL)}\Delta_{31}\frac{\sin(aL)}{aL}\Delta_{21}\cos(\Delta_{31}-\delta)$$
$$+\cos^2\theta_{23}\sin^2 2\theta_{12}\frac{\sin(aL)}{aL}\Delta_{21}^2$$

$$a = \frac{G_F N_e}{\sqrt{2}} \qquad \Delta_{ij} = \frac{\Delta m_{ij}^2 L}{4E}$$

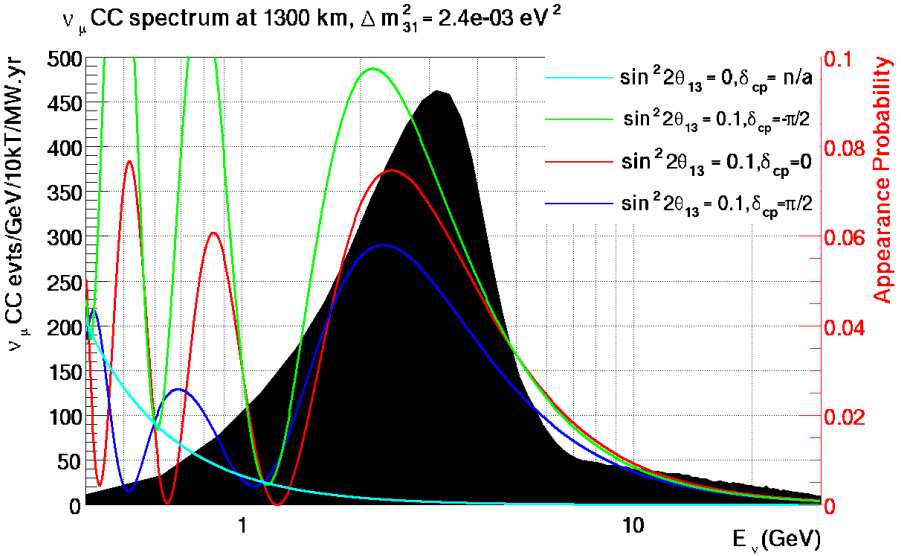

- ν_e appearance amplitude depends simultaneously on θ_{13}, θ_{23}, δ_{CP}, and matter effects –
- Measurements of all four possible in a single experiment.

ν_e appearance gives access to δ

$$P(\nu_\mu \to \nu_e) \approx \sin^2\theta_{23}\sin^2 2\theta_{13}\frac{\sin^2(\Delta_{31}-aL)}{(\Delta_{31}-aL)^2}\Delta_{31}^2$$
$$+\sin 2\theta_{23}\sin 2\theta_{13}\sin 2\theta_{12}\frac{\sin(\Delta_{31}-aL)}{(\Delta_{31}-aL)}\Delta_{31}\frac{\sin(aL)}{aL}\Delta_{21}\cos(\Delta_{31}-\delta)$$
$$+\cos^2\theta_{23}\sin^2 2\theta_{12}\frac{\sin(aL)}{aL}\Delta_{21}^2$$

$$a = \frac{G_F N_e}{\sqrt{2}}$$
$$\Delta_{ij} = \frac{\Delta m_{ij}^2 L}{4E}$$

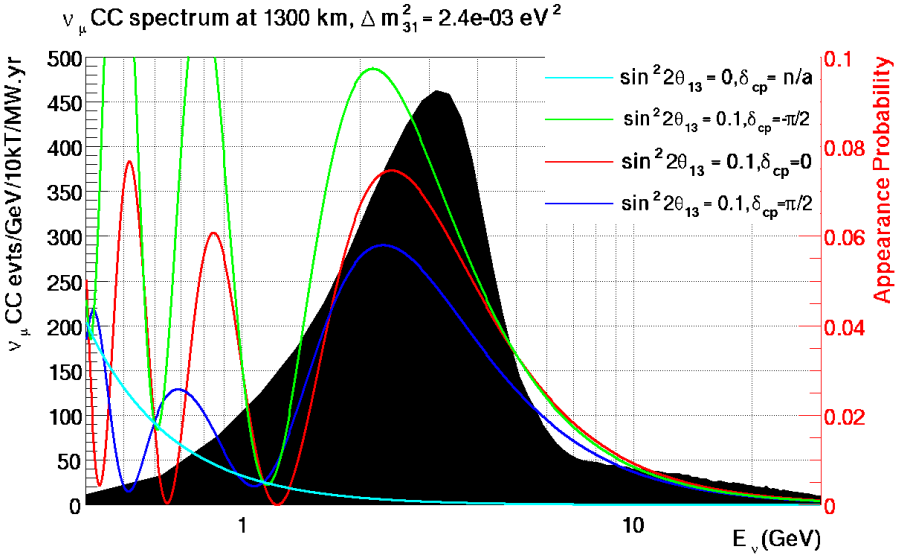

- ν_e appearance amplitude depends simultaneously on θ_{13}, θ_{23}, δ_{CP}, and matter effects –
- Measurements of all four possible in a single experiment.

ν_e appearance gives access to δ

$$P(\nu_\mu \to \nu_e) \approx \sin^2\theta_{23}\sin^2 2\theta_{13}\frac{\sin^2(\Delta_{31}-aL)}{(\Delta_{31}-aL)^2}\Delta_{31}^2$$
$$+\sin 2\theta_{23}\sin 2\theta_{13}\sin 2\theta_{12}\frac{\sin(\Delta_{31}-aL)}{(\Delta_{31}-aL)}\Delta_{31}\frac{\sin(aL)}{aL}\Delta_{21}\cos(\Delta_{31}-\delta)$$
$$+\cos^2\theta_{23}\sin^2 2\theta_{12}\frac{\sin(aL)}{aL}\Delta_{21}^2$$

$$a = \frac{G_F N_e}{\sqrt{2}} \qquad \Delta_{ij} = \frac{\Delta m_{ij}^2 L}{4E}$$

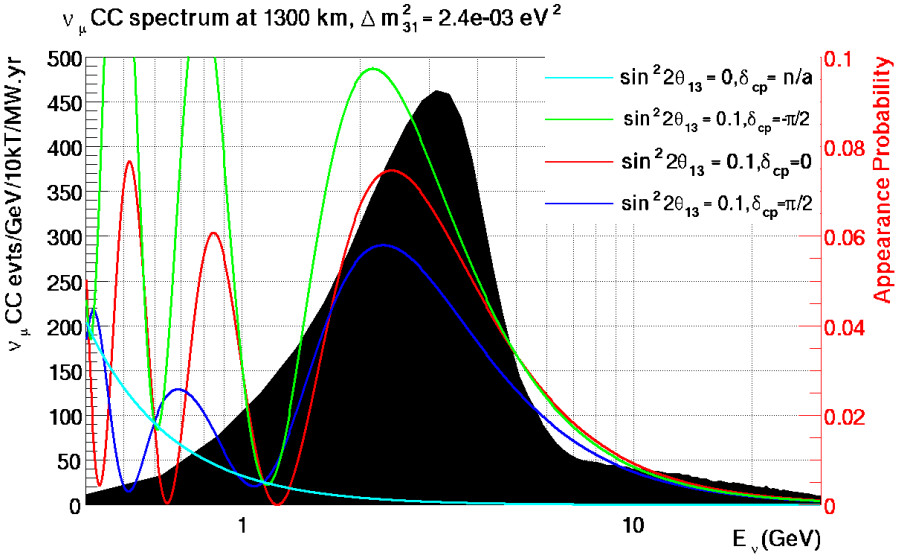

- ν_e appearance amplitude depends simultaneously on θ_{13}, θ_{23}, δ_{CP}, and matter effects –
- Measurements of all four possible in a single experiment.
- Need to resolve degeneracies (e.g., MO vs. CP).

ν_e appearance gives access to δ

$$P(\nu_\mu \to \nu_e) \approx \sin^2\theta_{23}\sin^2 2\theta_{13}\frac{\sin^2(\Delta_{31}-aL)}{(\Delta_{31}-aL)^2}\Delta_{31}^2$$
$$+\sin 2\theta_{23}\sin 2\theta_{13}\sin 2\theta_{12}\frac{\sin(\Delta_{31}-aL)}{(\Delta_{31}-aL)}\Delta_{31}\frac{\sin(aL)}{aL}\Delta_{21}\cos(\Delta_{31}-\delta)$$
$$+\cos^2\theta_{23}\sin^2 2\theta_{12}\frac{\sin(aL)}{aL}\Delta_{21}^2$$

$$a = \frac{G_F N_e}{\sqrt{2}} \qquad \Delta_{ij} = \frac{\Delta m_{ij}^2 L}{4E}$$

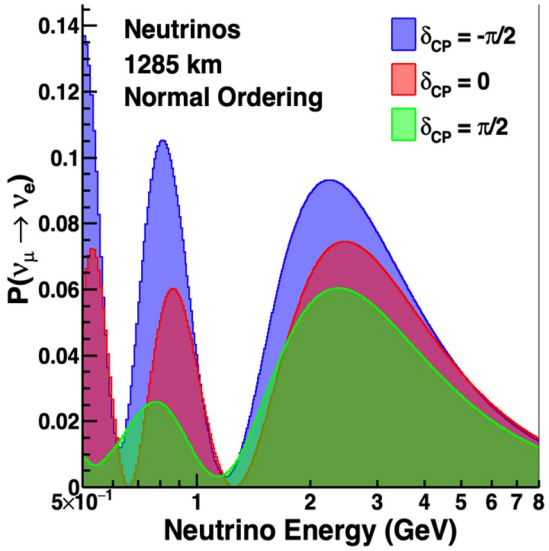

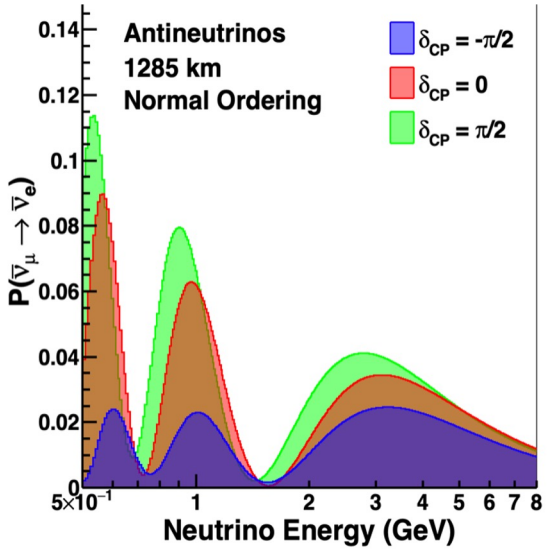

How to measure LBL neutrino oscillations

- Measure flavour change as a function of energy over a long distance.
- Starting with a muon-neutrino beam, we observe muon-neutrino disappearance and electron-neutrino appearance.
- Measure event rates and not the flux directly.
- Measurement is a convolution of the oscillation probabilities *P*, the neutrino flux Φ, the cross sections σ, and the detector response *T*.

$$\frac{N^{\mathrm{FD}}_{\nu_i}}{N^{\mathrm{ND}}_{\nu_\mu}}(E_{\mathrm{rec}}) = \frac{\int \Phi^{\mathrm{FD}}_{\nu_\mu}(E_\nu) \cdot P_{\nu_\mu \to \nu_i}(E_\nu) \cdot \sigma^{\mathrm{Ar}}_{\nu_i} \cdot T^{\mathrm{FD}}_{\nu_i}(E_\nu, E_{\mathrm{rec}})\, \mathrm{d}E_\nu}{\int \Phi^{\mathrm{ND}}_{\nu_\mu}(E_\nu) \cdot \sigma^{\mathrm{X}}_{\nu_\mu} \cdot T^{\mathrm{ND}}_{\nu_\mu}(E_\nu, E_{\mathrm{rec}})\, \mathrm{d}E_\nu}$$

DUNE in a Nutshell

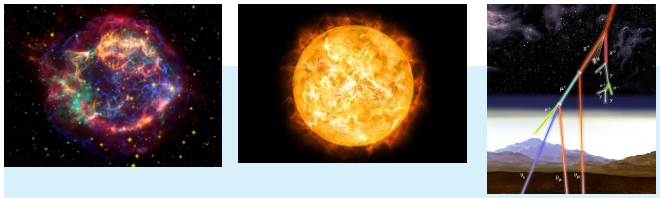

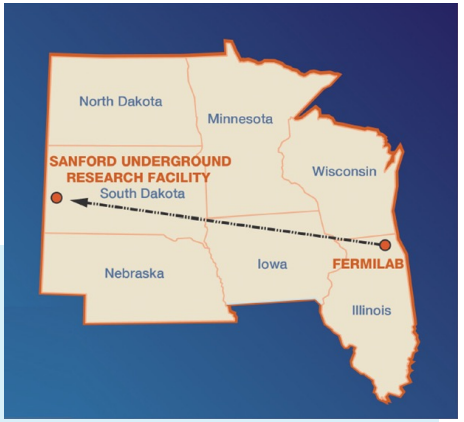

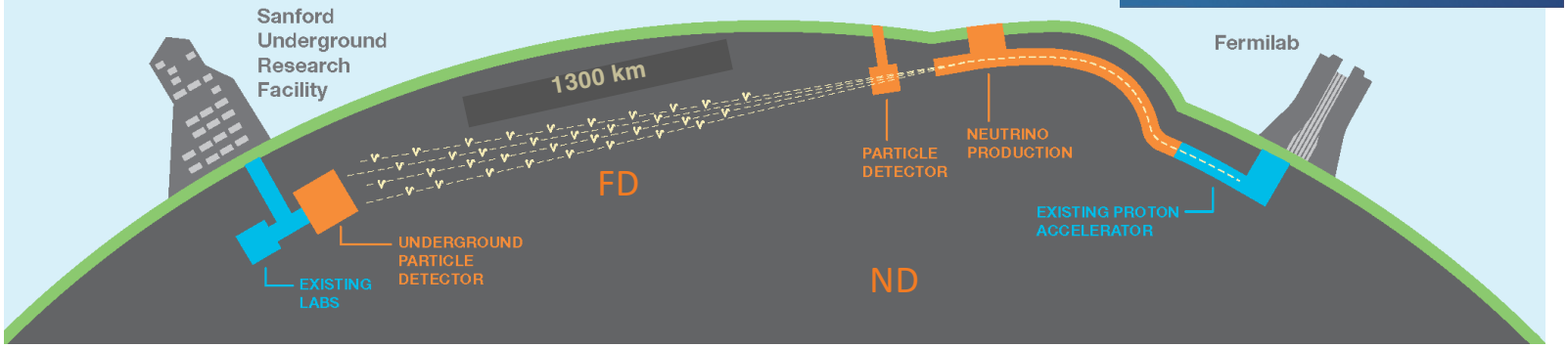

1. A high-power, wide-band **neutrino beam** (~ GeV energy range).
2. A ≈ 70 kt **liquid-argon Far Detector** in South Dakota, located 1478 m underground in a former gold mine.
3. A **Near Detector** located approximately 575 m from the neutrino source at Fermilab close to Chicago.

Proton Improvement Plan (PIP-II)

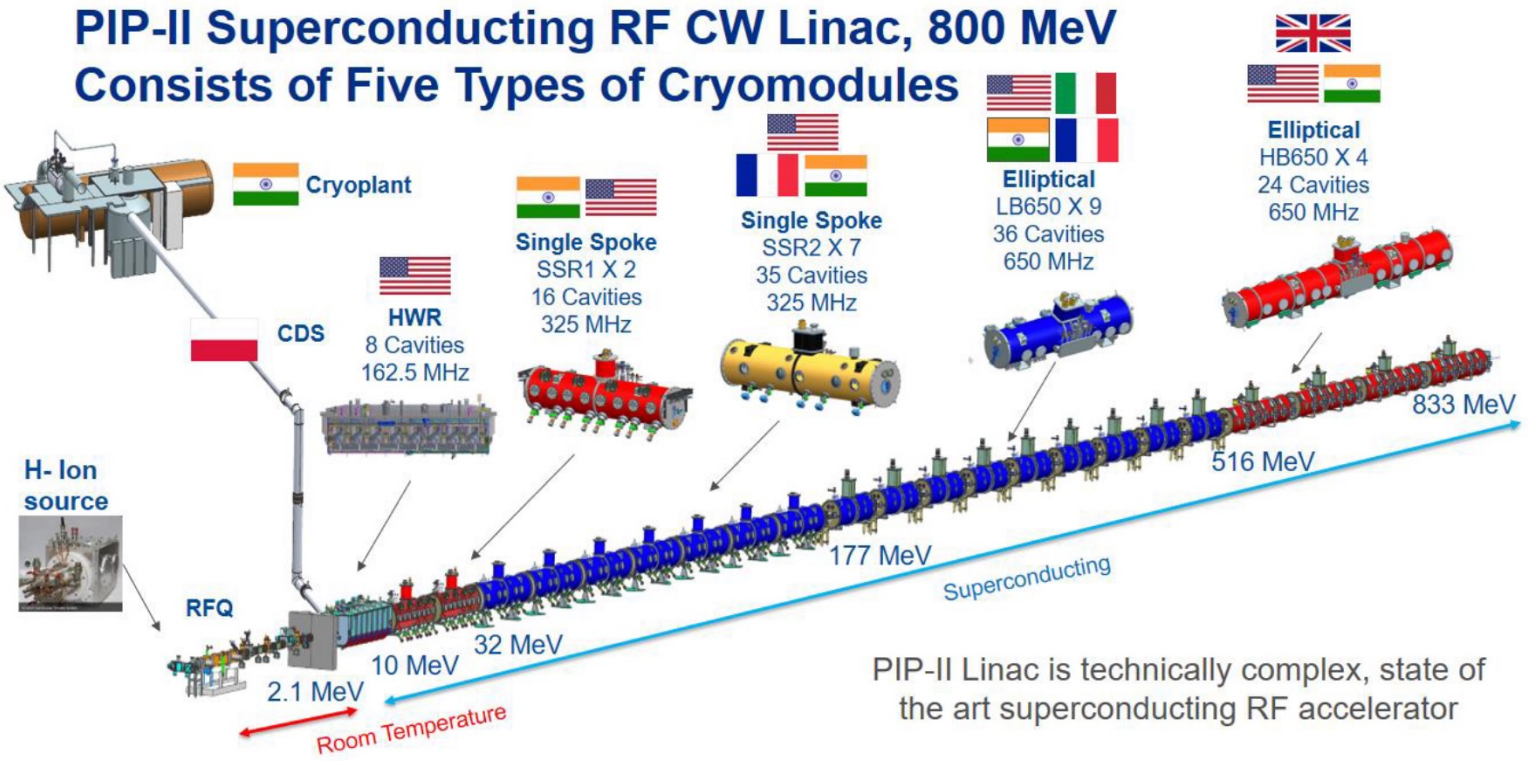

Proton Improvement Plan (PIP-II)

4850L Facilities

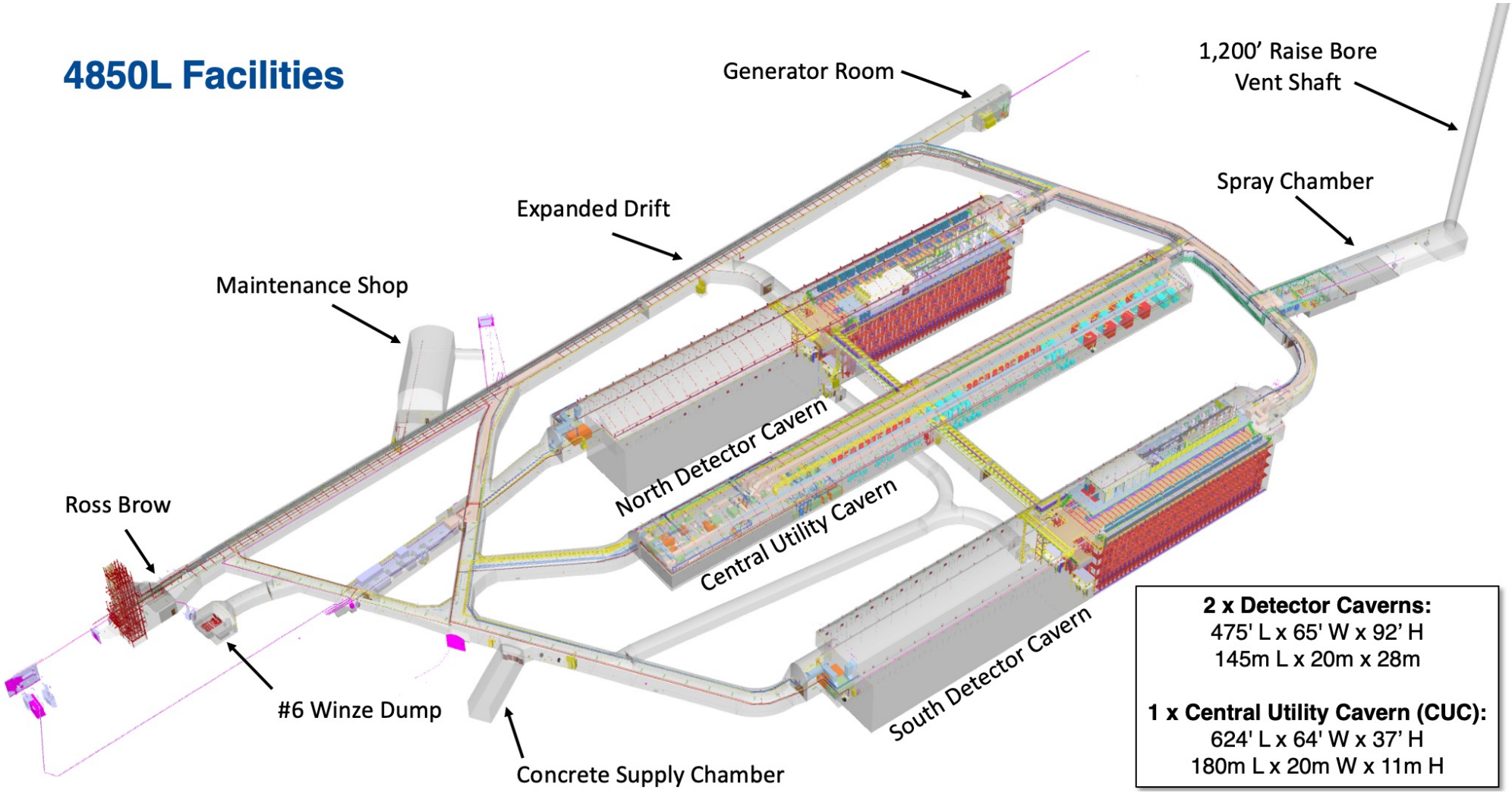

2 x Detector Caverns:
475' L x 65' W x 92' H
145m L x 20m x 28m

1 x Central Utility Cavern (CUC):
624' L x 64' W x 37' H
180m L x 20m W x 11m H

12 Feb 2022

Central Utility Cavern Pilot Drift Breakthrough

Cavern is being constructed

Nigel Lockyer
@Nigel_Lockyer

Look carefully, the construction worker says he has just started excavating this cavern. The final enormous size is hard to comprehend. All for neutrinos.

2:27 pm · 2 Jul 2022 · Twitter for iPhone

Module 1: Horizontal Drift

Home > News > UK scientists build core components of global neutrino experiment

UK scientists build core components of global neutrino experiment

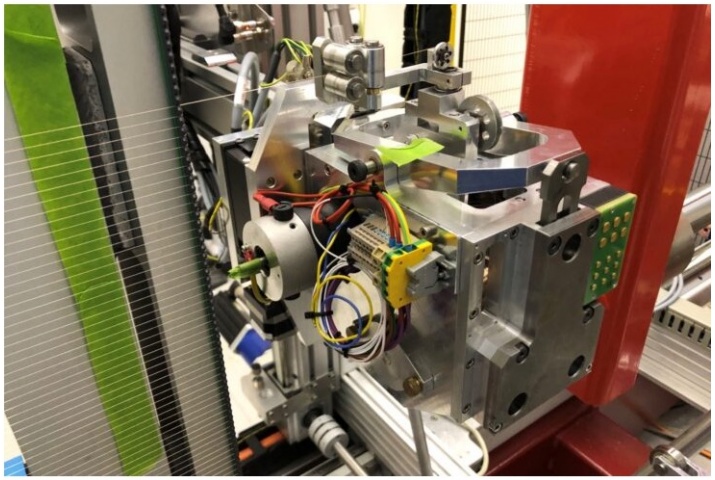

Related content

⇨ About ProtoDUNE

Subscribe to UKRI emails

Sign up for news, views, events a
funding alerts.

Email address

Subscribe

- 150 Anode Plane Assemblies (APA)
- 130 in UK and 20 in US

ProtoDUNE at CERN

Module 2: Vertical Drift

Successful tests at CERN, leading to design of ProtoDUNE Module-0 for Vertical Drift.

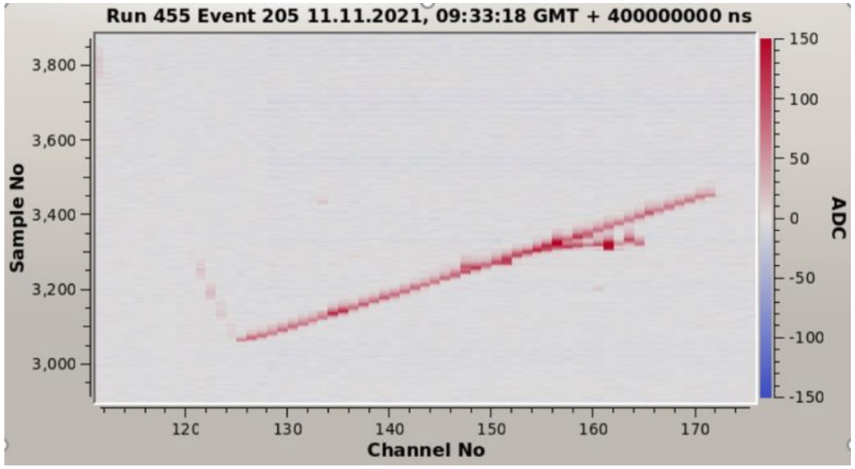

A ProtoDUNE-HD Data Event

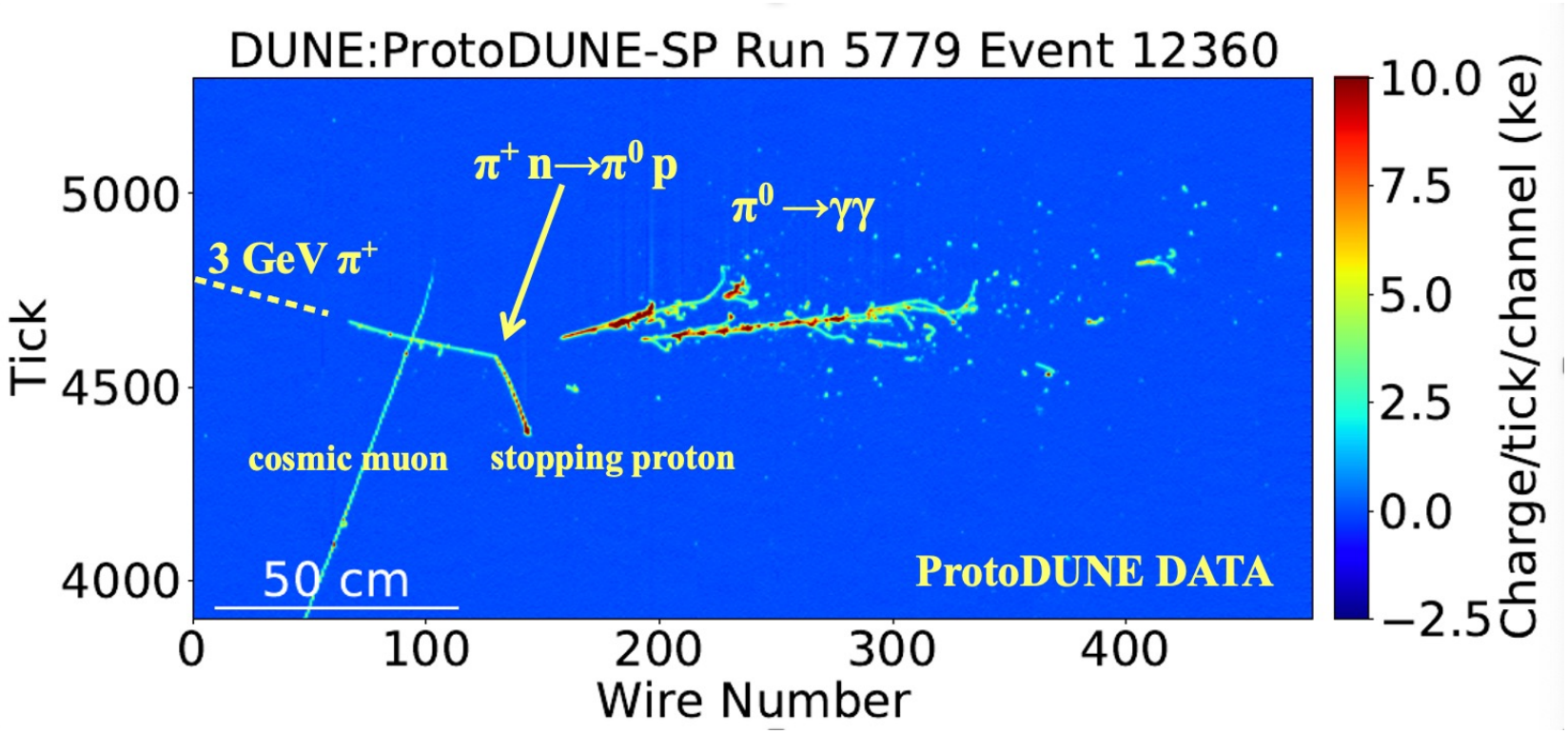

Reconstruction of events performed by PANDORA framework with the use of Grid computing resources, both areas UK-led.

DUNE Phase I Near Detector

We expect to replace TMS by a gas-argon TPC for Phase-II.

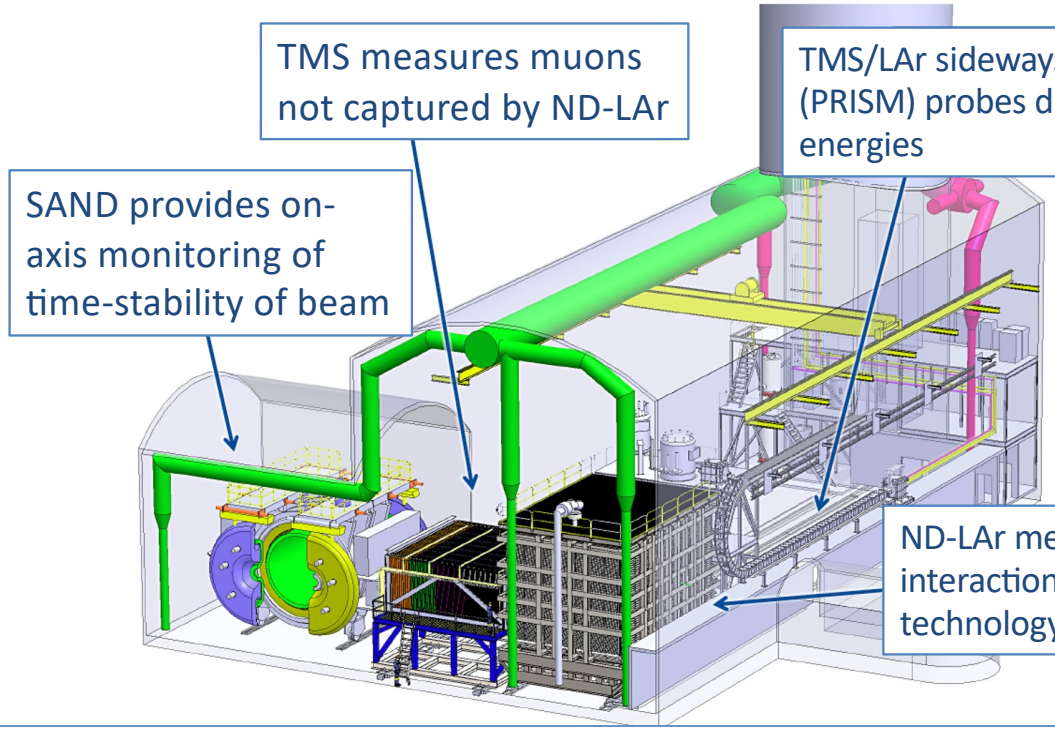

Systematics

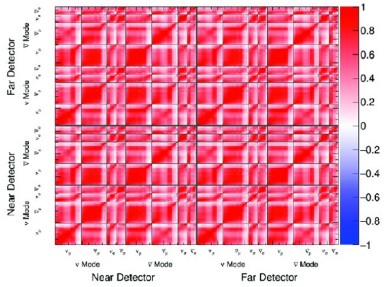

- Near Detectors constrain systematic uncertainties for long-baseline oscillation analysis
  Neutrino flux & cross-section, and detector systematics
- In addition, >100 million interactions will also enable a rich non-oscillation physics programme (e.g. BSM).

DUNE PRISM

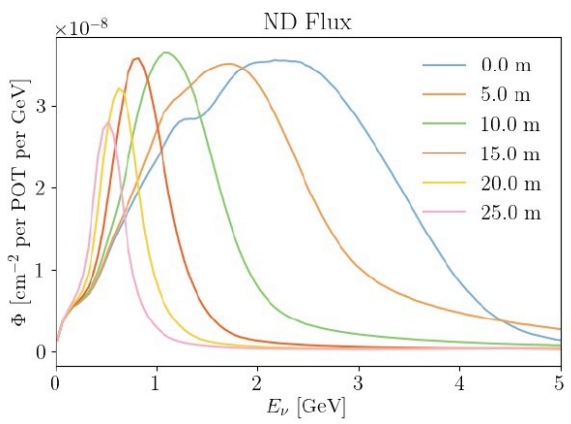

x

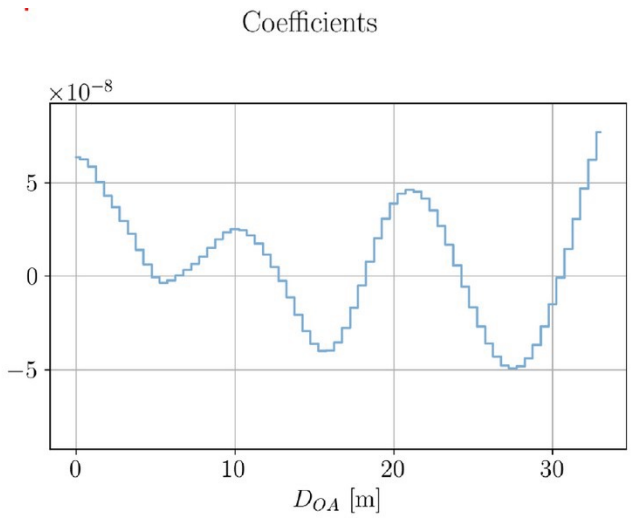

→

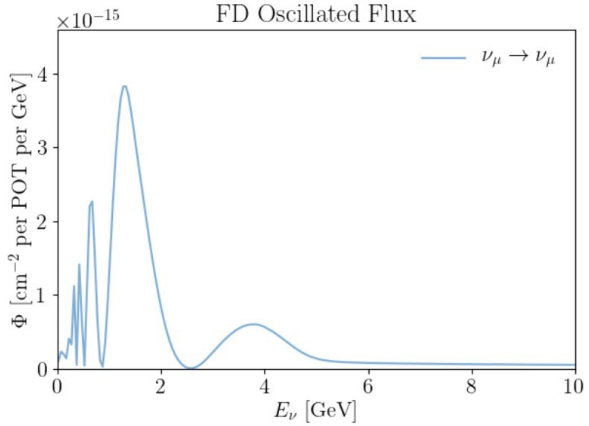

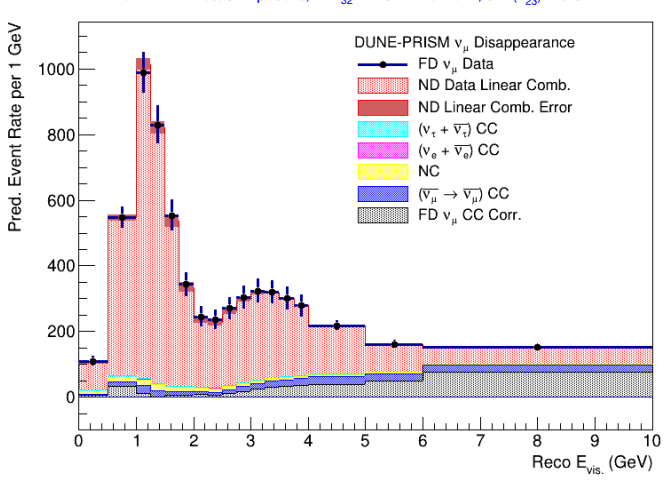

- FD flux ≠ ND flux → uncertainties in energy extrapolation
- ND flux changes with angle due to pion decay kinematics
- Take ND data in different fluxes → build linear combination to match FD oscillated spectra
- Robust analysis approach with very minimal x
- dependence on interaction modeling

DUNE PRISM

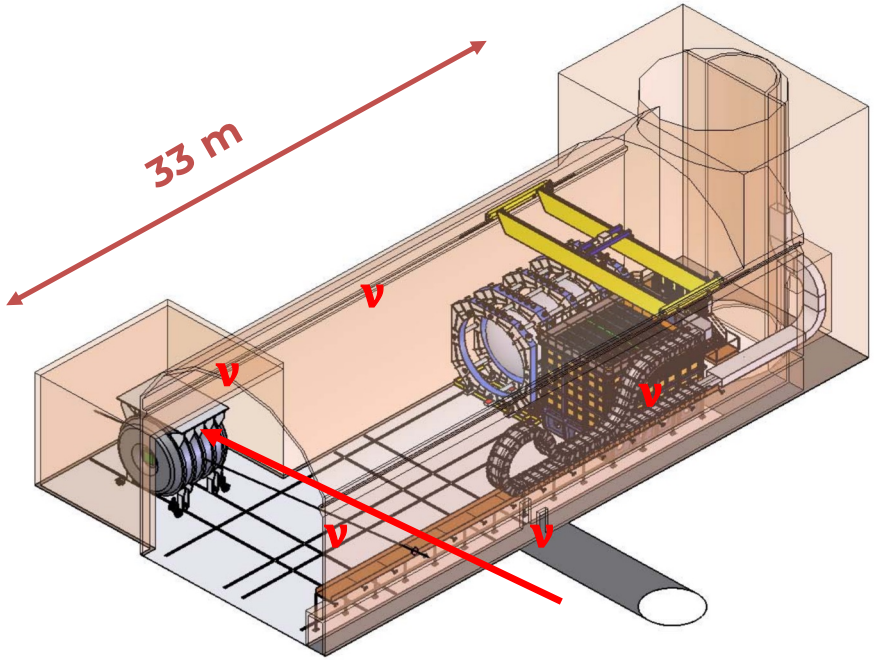
33 m
ν
ν
ν
ν
ν

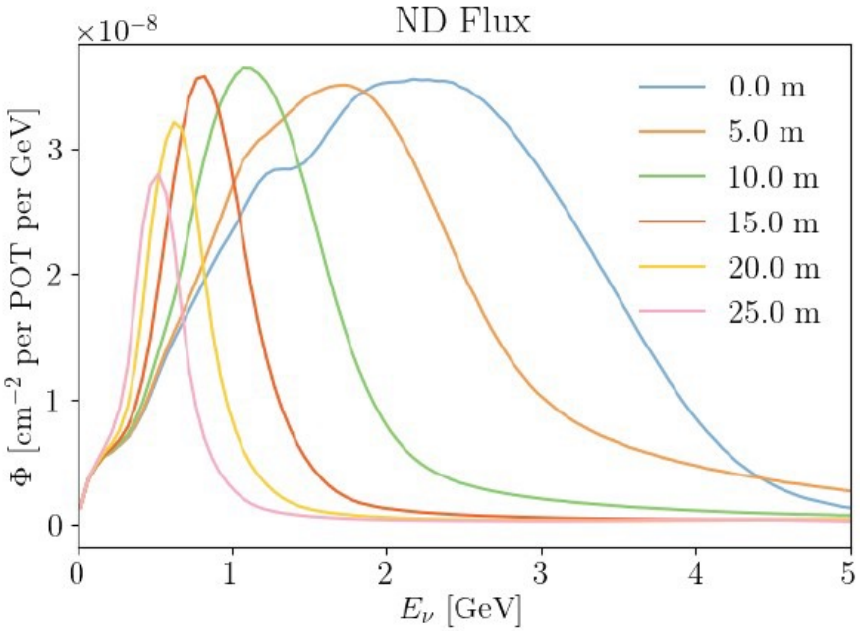
ND Flux
×10⁻⁸
Φ [cm⁻² per POT per GeV]
Eν [GeV]
0.0 m
5.0 m
10.0 m
15.0 m
20.0 m
25.0 m
0
1
2
3
4
5

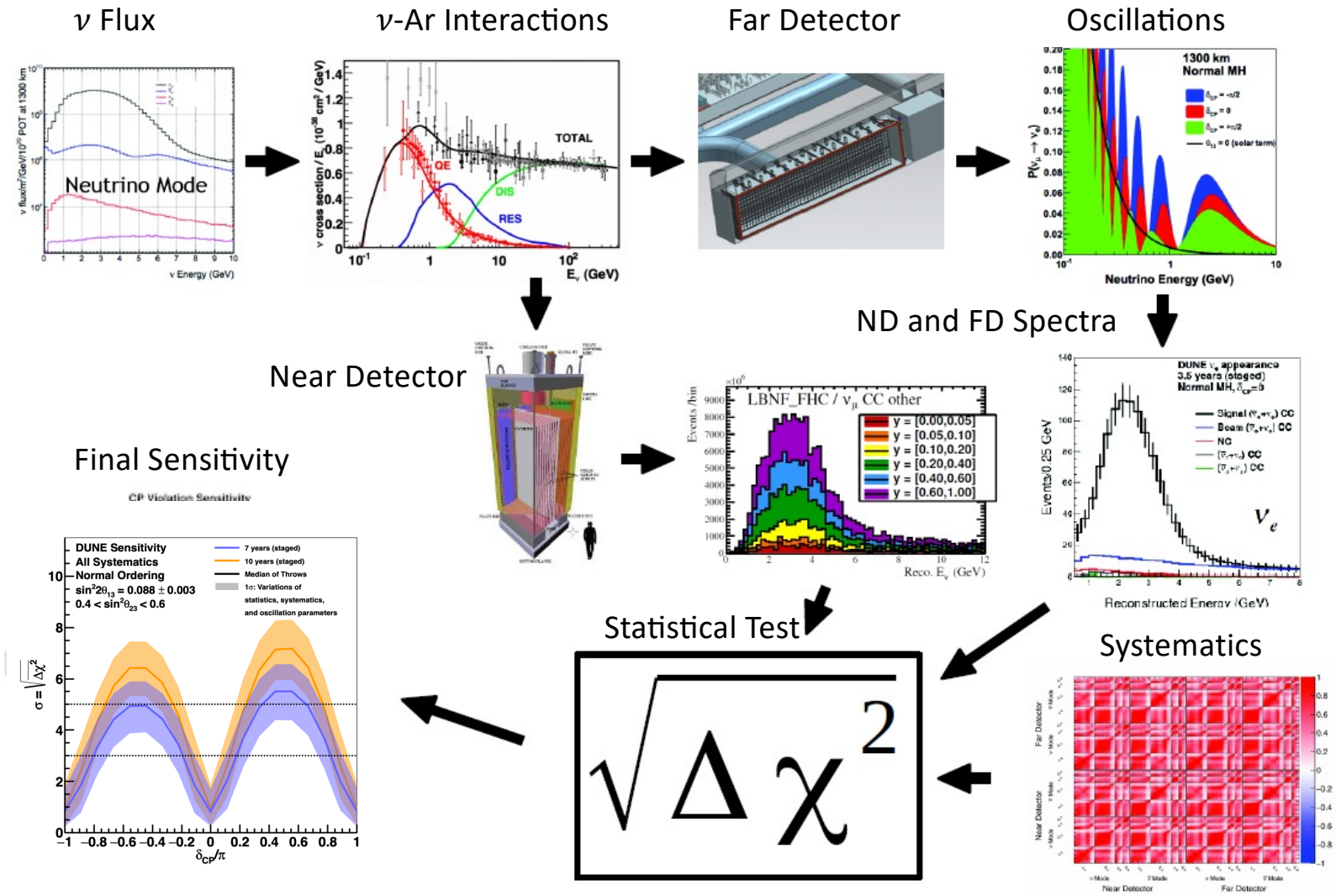
ν Flux
ν-Ar Interactions
Far Detector
Oscillations
Neutrino Mode
ν Energy (GeV)
TOTAL
QE
DIS
RES
E_ν (GeV)
1300 km
Normal MH
Neutrino Energy (GeV)
ND and FD Spectra
Near Detector
LBNF_FHC / ν_μ CC other
y = [0.00,0.05]
y = [0.05,0.10]
y = [0.10,0.20]
y = [0.20,0.40]
y = [0.40,0.60]
y = [0.60,1.00]
Reco. E_ν (GeV)
DUNE ν_e appearance
3.5 years (staged)
Normal MH, δ_CP=0
Signal
Beam
NC
CC
ν_e
Reconstructed Energy (GeV)
Final Sensitivity
CP Violation Sensitivity
DUNE Sensitivity
All Systematics
Normal Ordering
sin²2θ13 = 0.088 ± 0.003
0.4 < sin²θ23 < 0.6
7 years (staged)
10 years (staged)
Median of Throws
1σ: Variations of statistics, systematics, and oscillation parameters
δCP/π
Statistical Test
Systematics
Near Detector
Far Detector

DUNE ν_μ disappearance & ν_e appearance

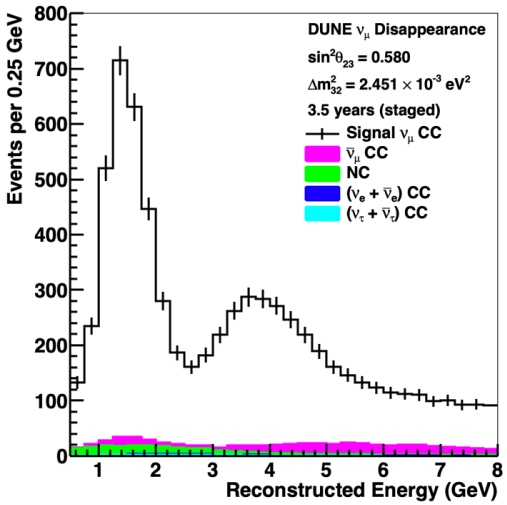

ν_μ

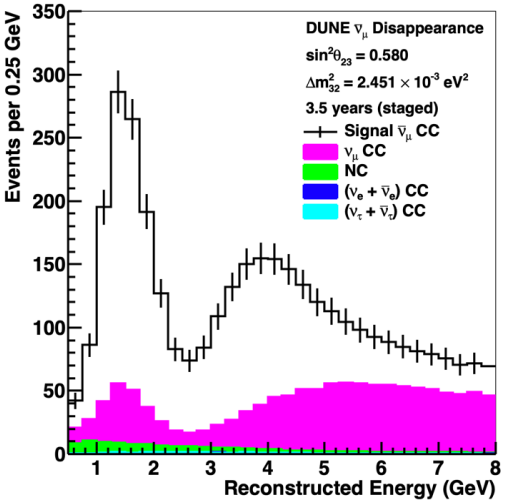

anti-ν_μ

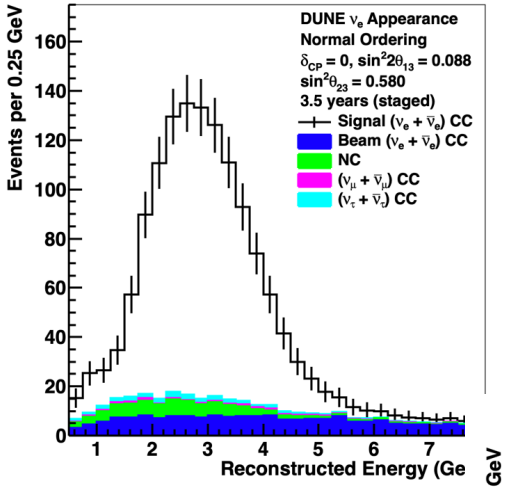

ν_e

anti-ν_e

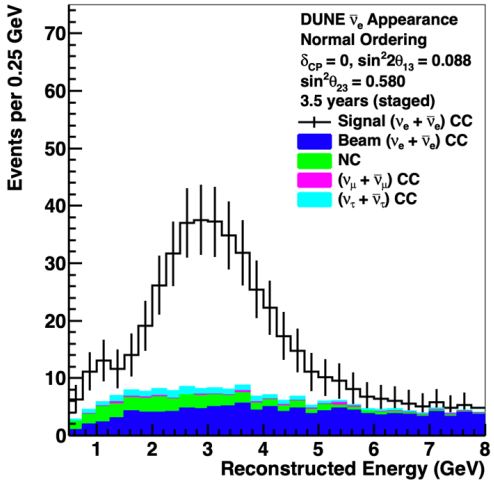

DUNE simulation

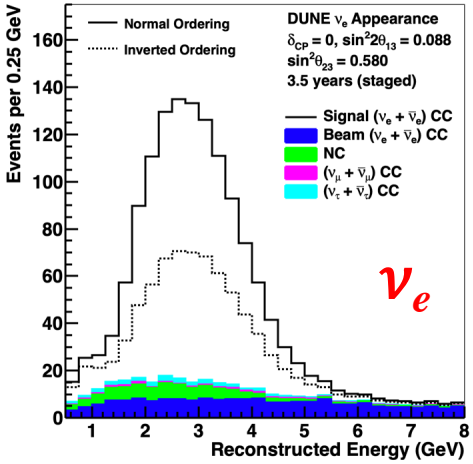

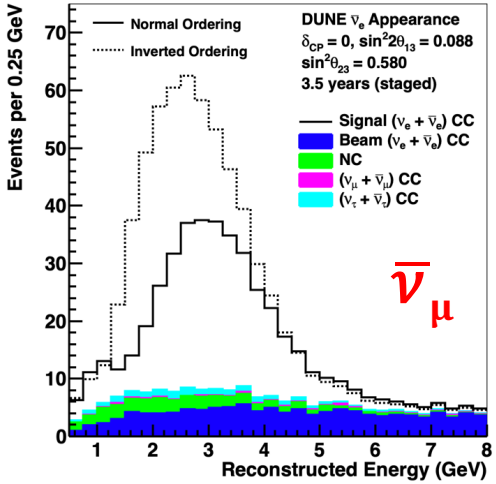

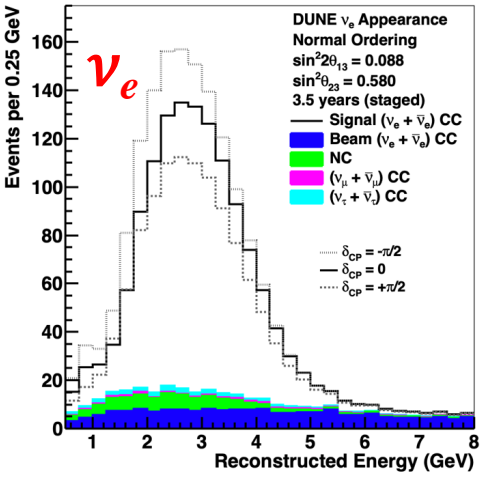

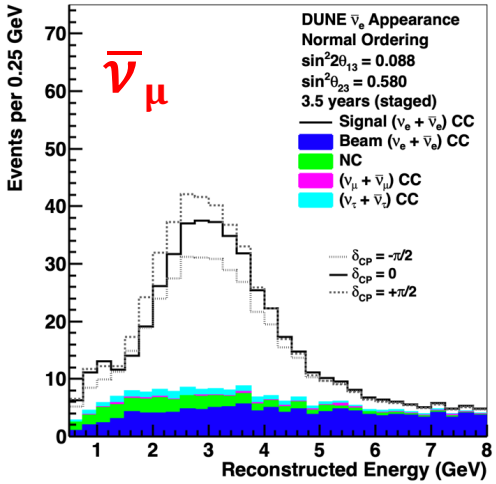

7 years

variation with mass ordering

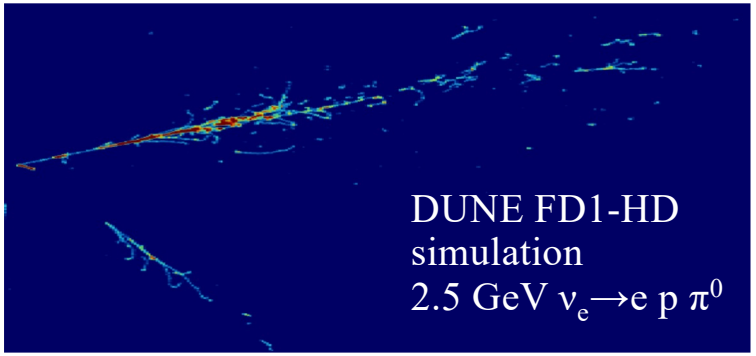

variation with δ_{CP}

DUNE: Sensitivity to CP Violation

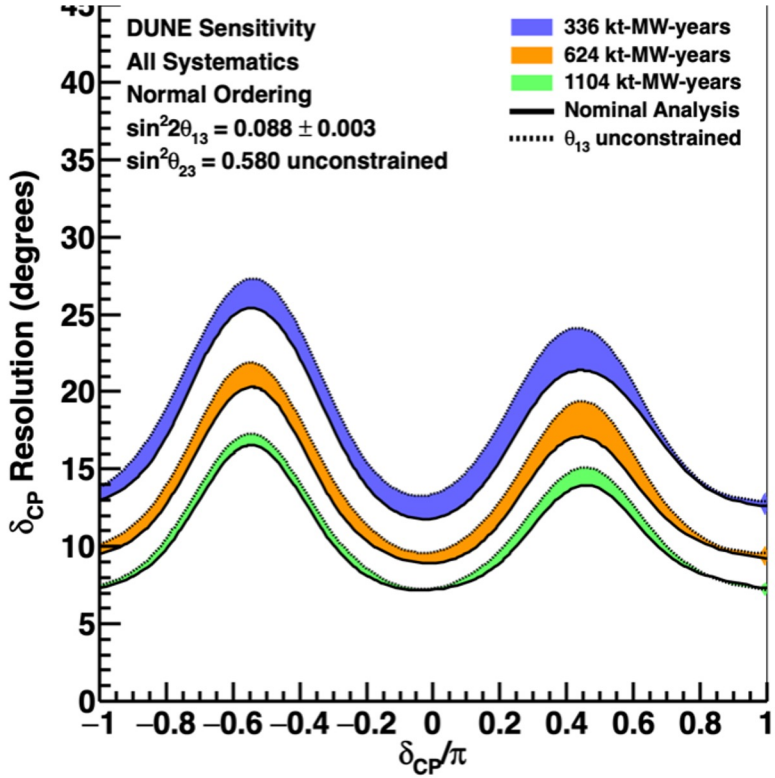

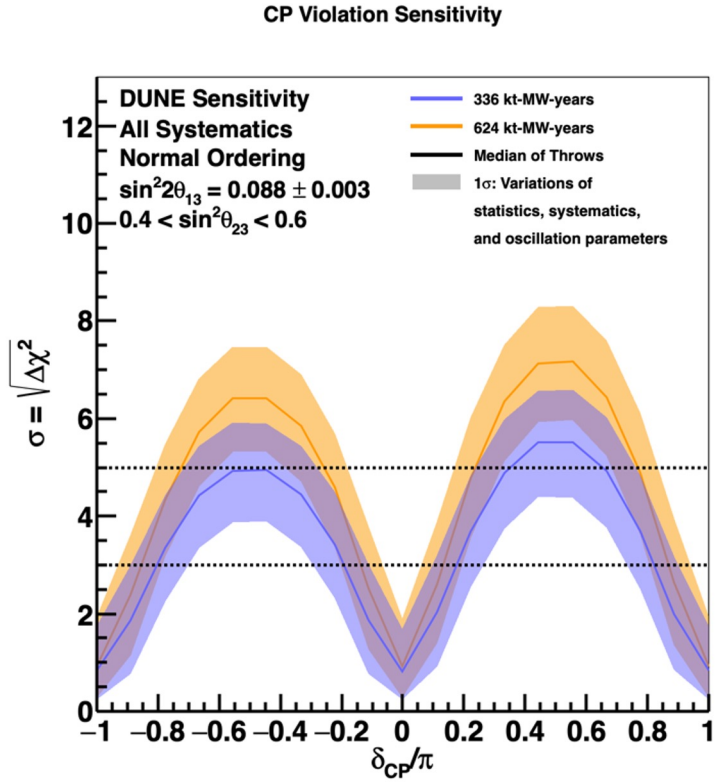

- 5σ discovery potential for CP violation over >50% of δ_{CP} values
- 7-16° resolution to δ_{CP}, *without reliance on other experiments*

DUNE: Sensitivity to Mass Ordering

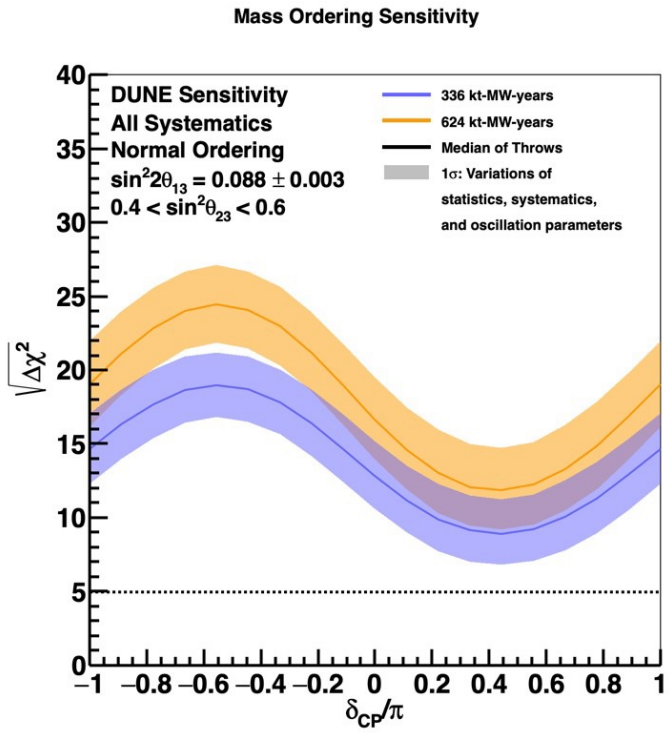

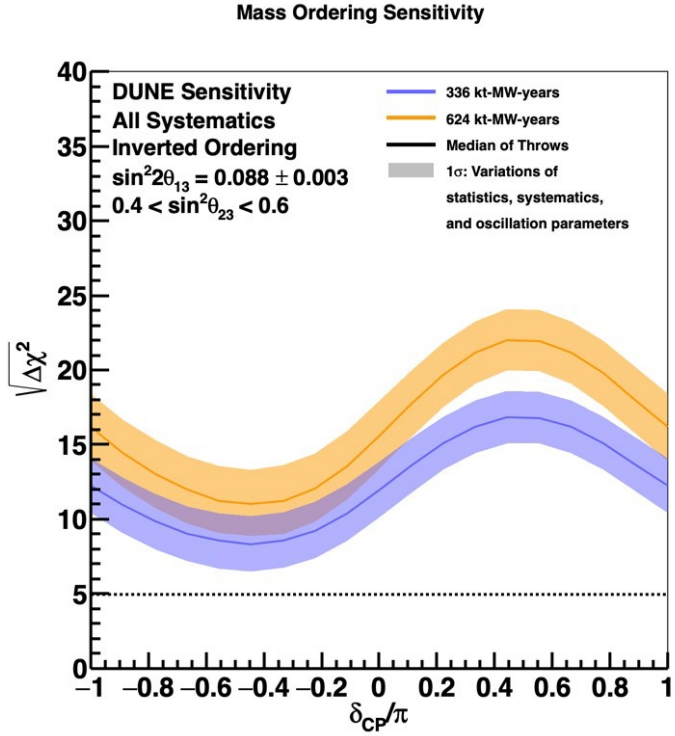

Regardless of the values of other parameters, and without dependence on other experiments, DUNE has unprecedented and unrivaled ability to definitively resolve the mass ordering

DUNE: Unitarity tests

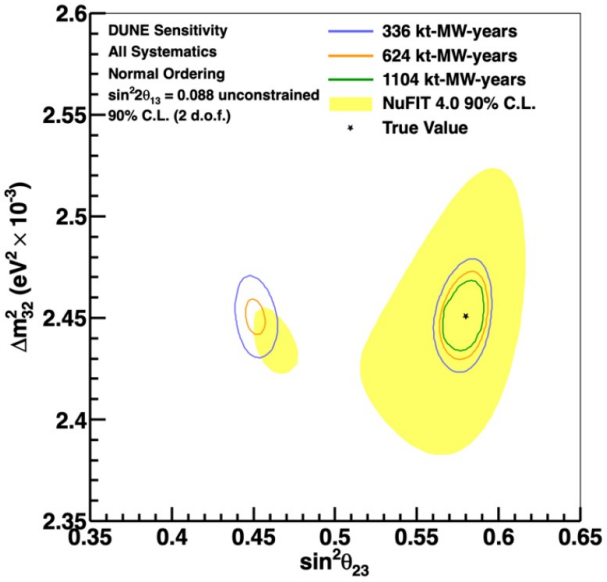

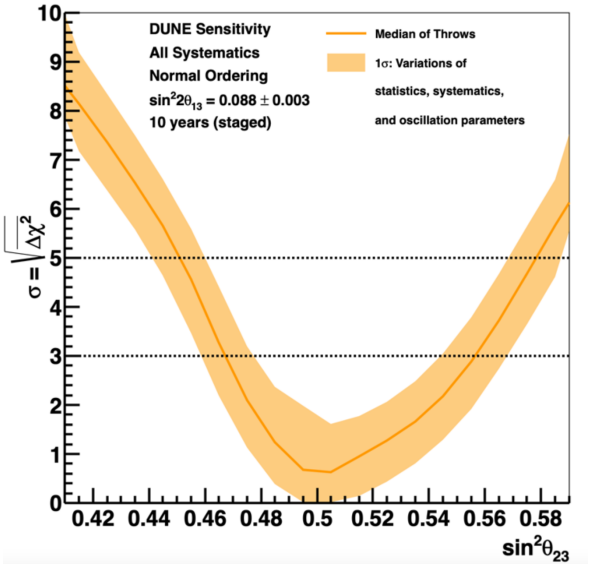

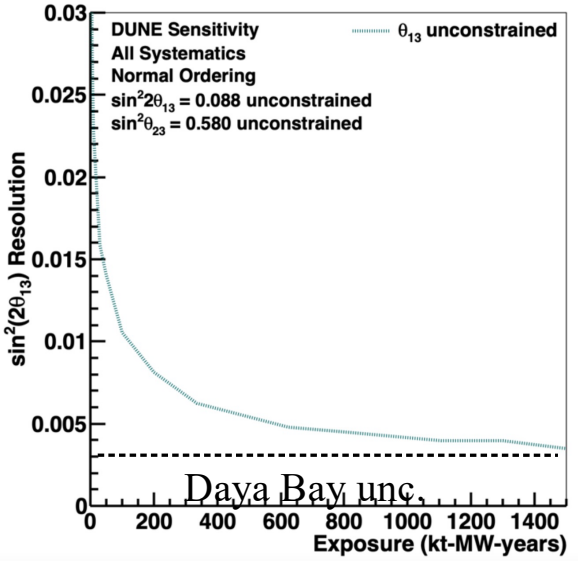

- World-leading precision on Δm^2_{32} and θ_{23}, including octant, and novel PRISM technique that is less sensitive to systematic effects
- Ultimate reach does not depend on external θ_{13} measurements, and comparison with reactor data directly tests PMNS unitarity

HyperKamiokande in a Nutshell

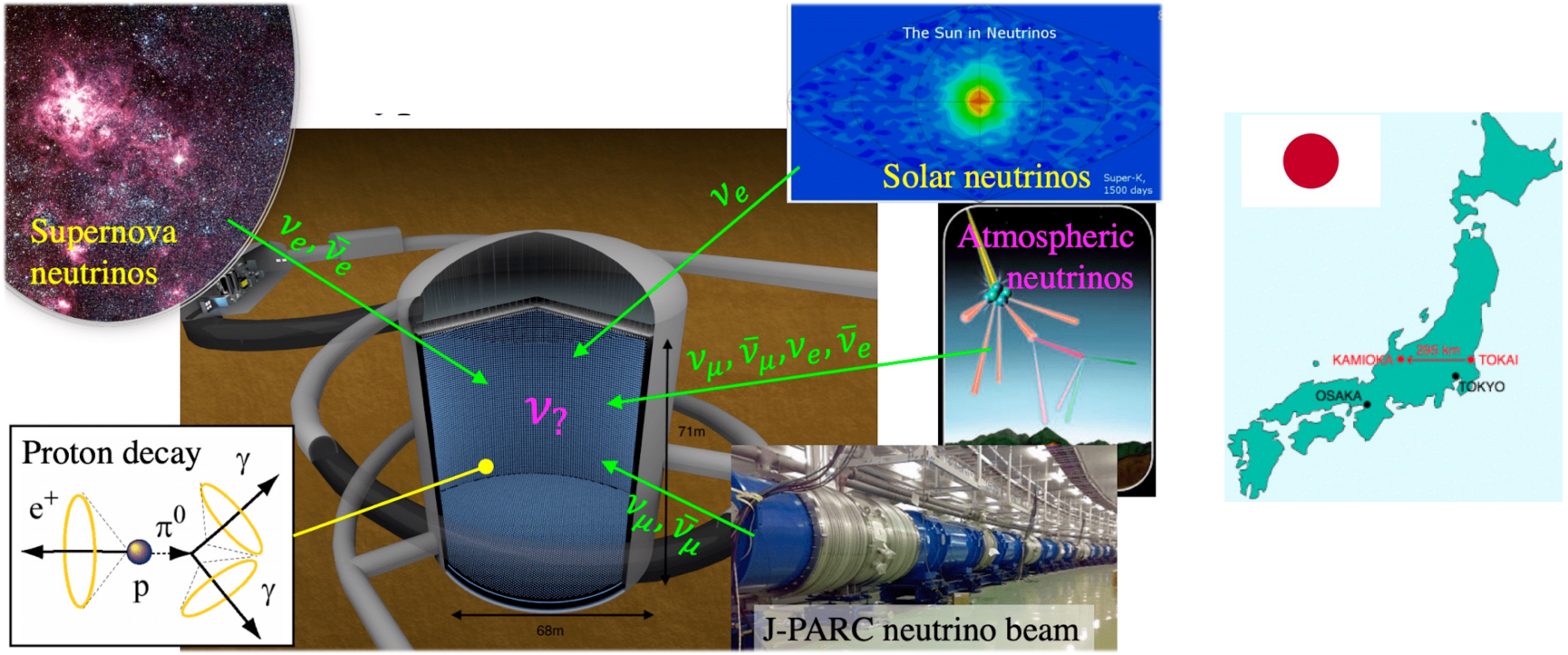

- **8.4 times larger fiducial mass** (190 kiloton) than SK with **double-sensitivity PMTs**
- New (IWCD) and upgraded (@280m) Near Detectors to control systematic uncertainties.
- J-PARC neutrino beam to be upgraded from 0.5 to 1.3 MW

HK Access Tunnel

Commissioning 2026
Far Detector operation in 2026

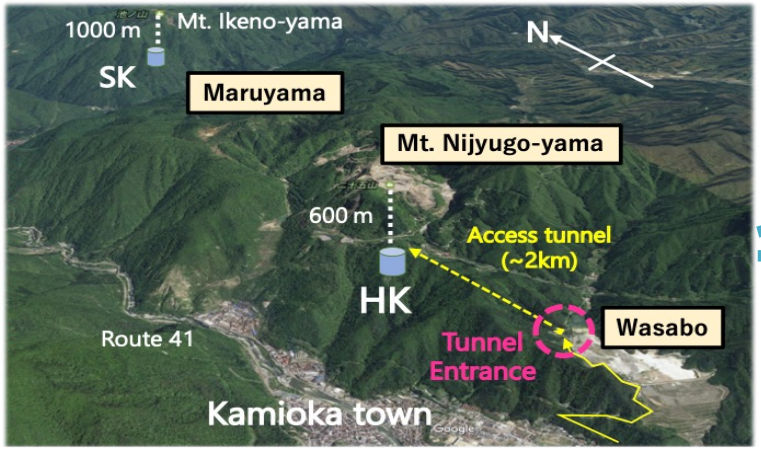

Access tunnel (1873 m) completed in February 2022 and work on approach tunnel has started.

HK: Sensitivity to CP Violation

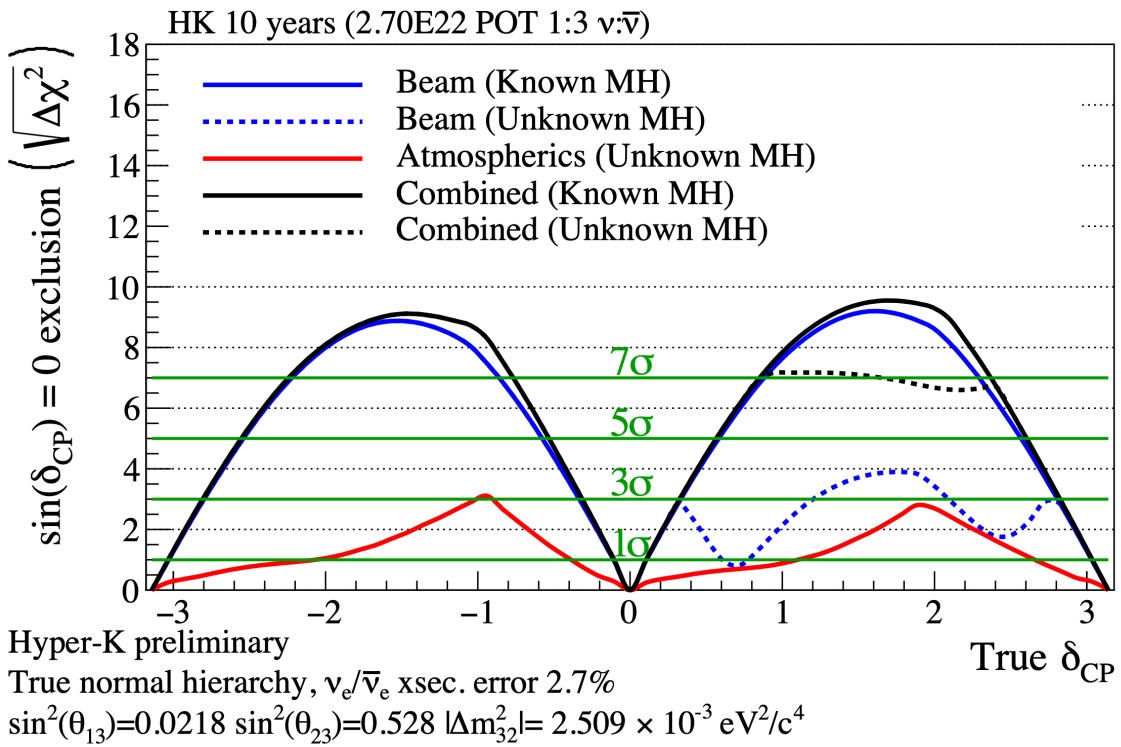

- Due to short baseline HK cannot resolve MO/CP degeneracy.
- If MO unknown, beam analysis less sensitive for some values of δ.
- Joint atmospheric and beam analysis increases sensitivity.

Other mass hierarchy measurements

JUNO: Snowmass2021 JUNO LOI

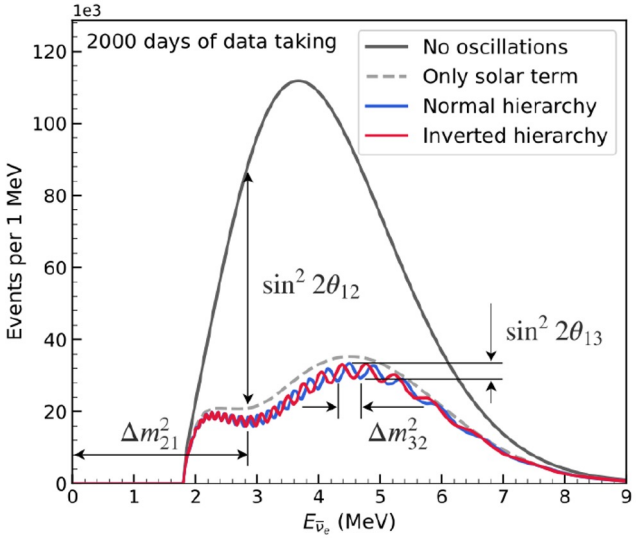

Super-K: PTEP Vol. 2019, Iss. 5 (2019)

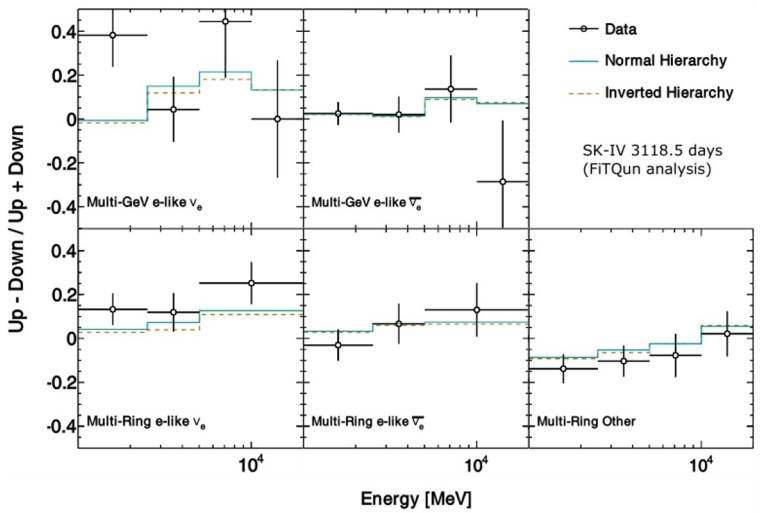

- JUNO can determine mass ordering by differentiating rapid wiggle with unprecedented energy resolution.
- Large water Cherenkov detectors can model ν_e/ν_e flux and cross sections and look for a small differences in the up/down asymmetry

CP Violation Phase

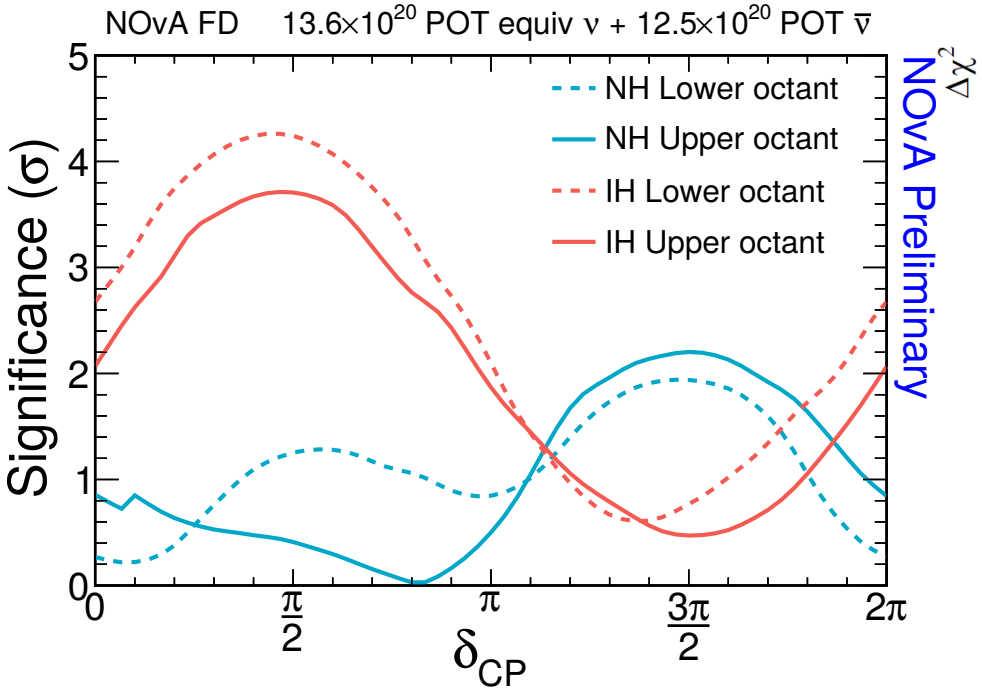

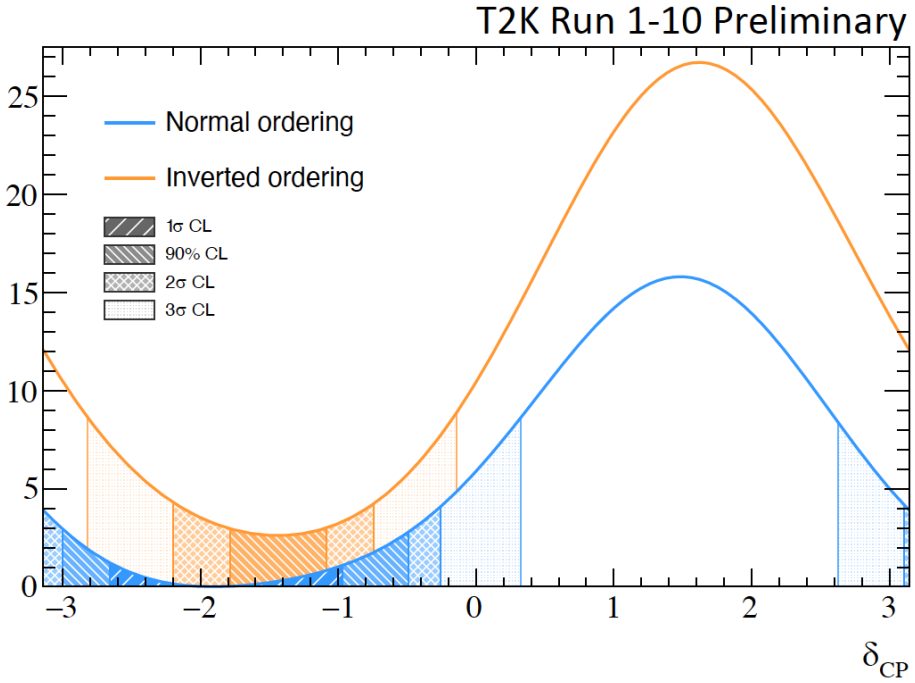

- Sensitivity to combination of CP phase and MO
- Normal ordering slightly preferred (1σ)
- Exclude IO, $\delta = \pi/2$ at > 3σ
- Disfavour NO, $\delta = 3\pi/2$ at ~2σ

- Using θ_{13} from reactor experiments
- CP conversation (0,π) excluded at 90% confidence level
- Normal ordering preferred

NOvA and T2K

- NOvA does not see strong neutrino/antineutrino asymmetry in electron neutrino appearance.
- T2K observes more electron neutrino appearance than electron antineutrino appearance.
- Current data are inconclusive – expect some improvements with further running.
- Need next-generation experiments to discover CPV and resolve mass ordering.

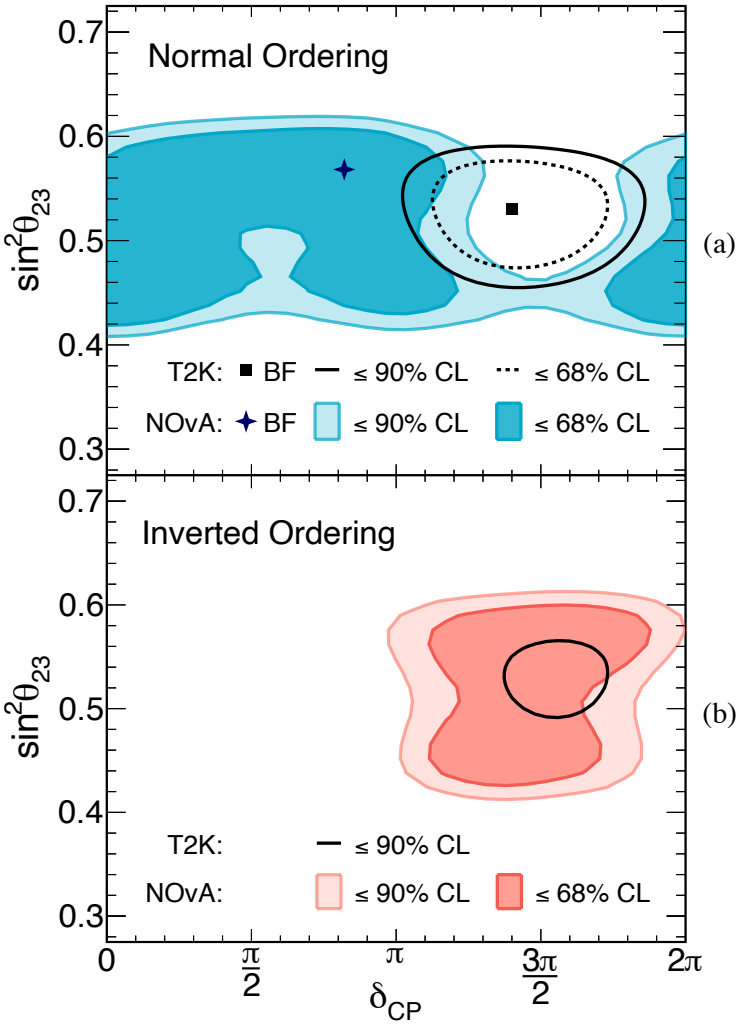

DUNE Phases

DUNE Phase I:

- Ramp up to 1.2 MW beam intensity
- Two 17kt LAr TPC FD modules
- Near detector: ND-LAr + TMS (movable) + SAND

DUNE Phase II:

- Fermilab proton beam upgrade to 2.4 MW
- Four 17kt LAr TPC FD modules
- Near detector: ND-LAr + ND-GAr (movable) + SAND

Phase II – full DUNE

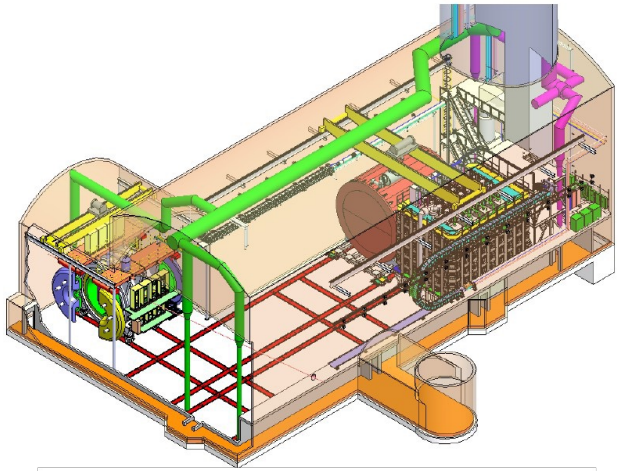

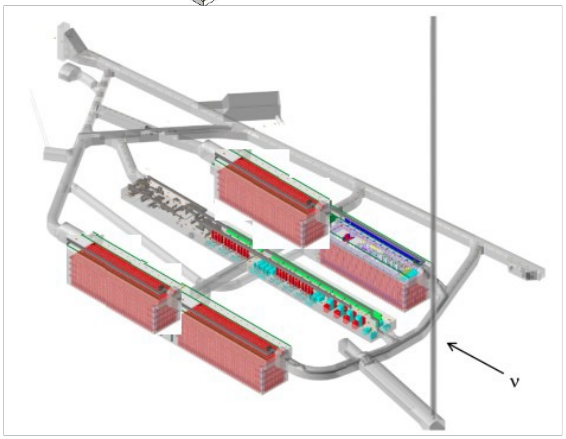

DUNE Phase I

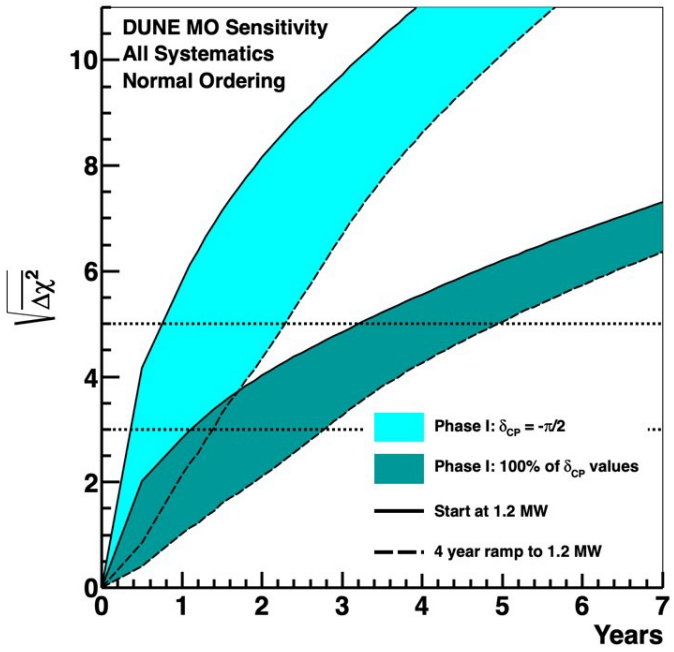

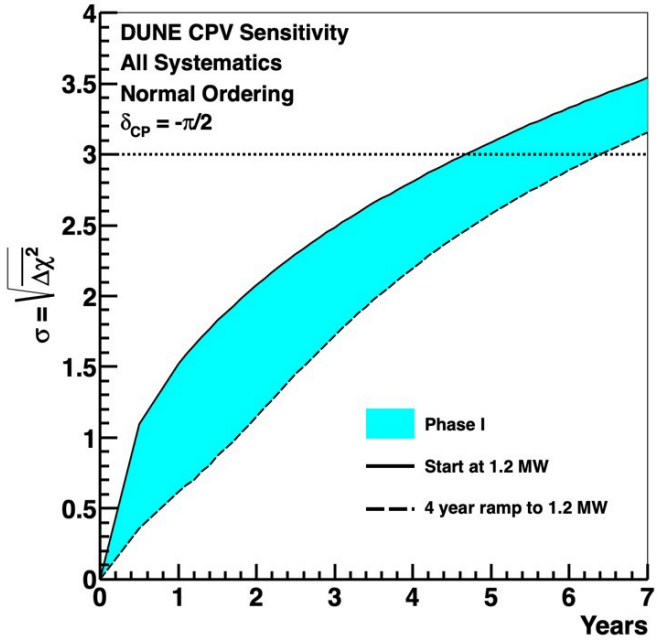

- Only experiment with 5σ mass ordering capability regardless of true parameters
- Discovery of CPV at 3σ if CP violation is large
- World-leading precision on Δm^2_{32}, and other oscillation measurements

DUNE Phase II

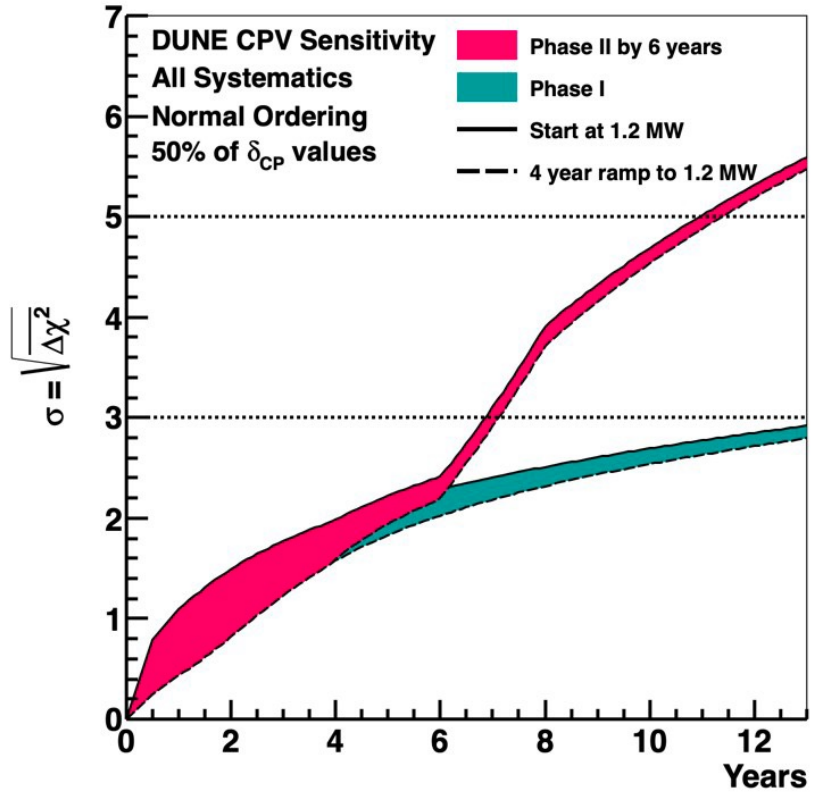

- DUNE needs full Phase II scope to achieve precision physics goals defined in P5 report
- Timescale for precision physics is driven by achieving full scope on aggressive timescale, early ramp-up is not as relevant
- A second phase of DUNE (Modules 3 and 4) can also extend physics capabilities, e.g. solar neutrinos or neutrinoless DBD.

DUNE Phase II

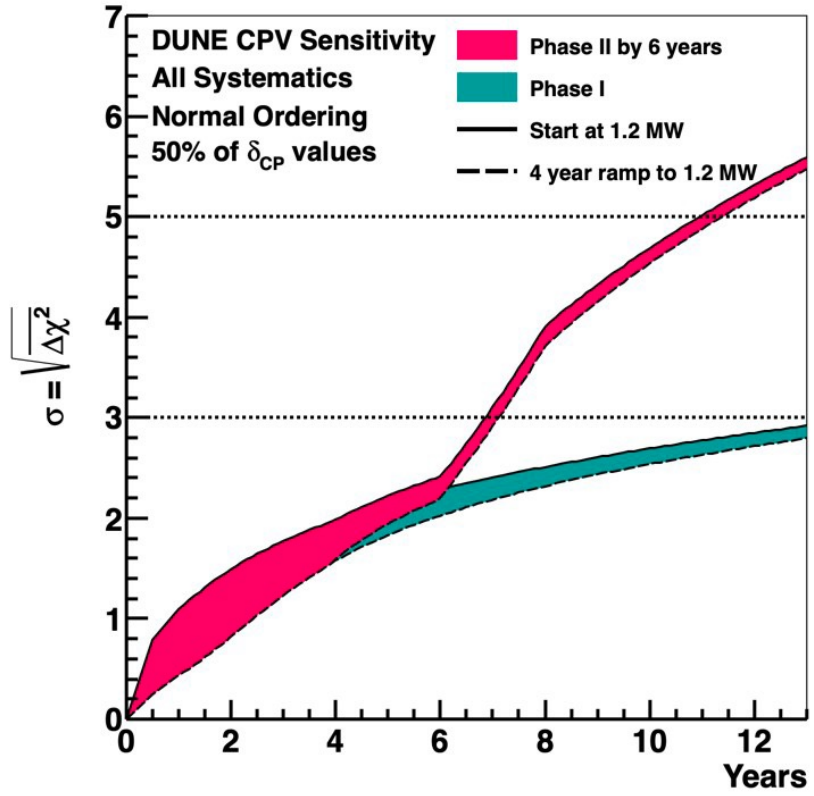

- DUNE needs full Phase II scope to achieve precision physics goals defined in P5 report
- Timescale for precision physics is driven by achieving full scope on aggressive timescale, early ramp-up is not as relevant
- A second phase of DUNE (Modules 3 and 4) can also extend physics capabilities, e.g. solar neutrinos or neutrinoless DBD.

DUNE Phase II

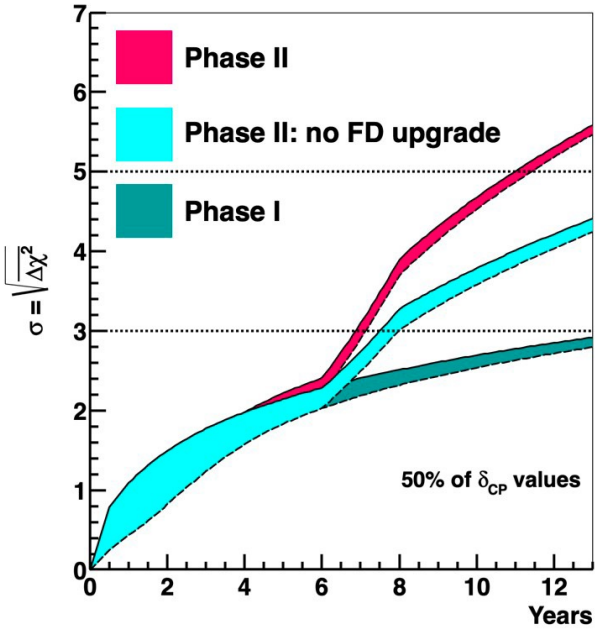

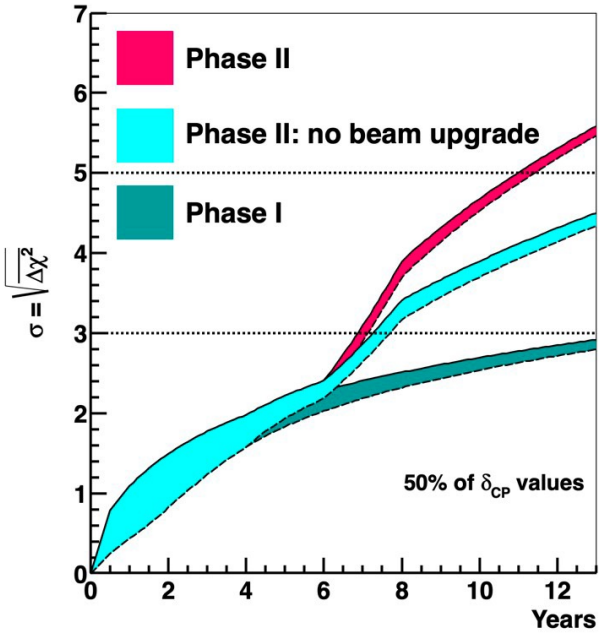

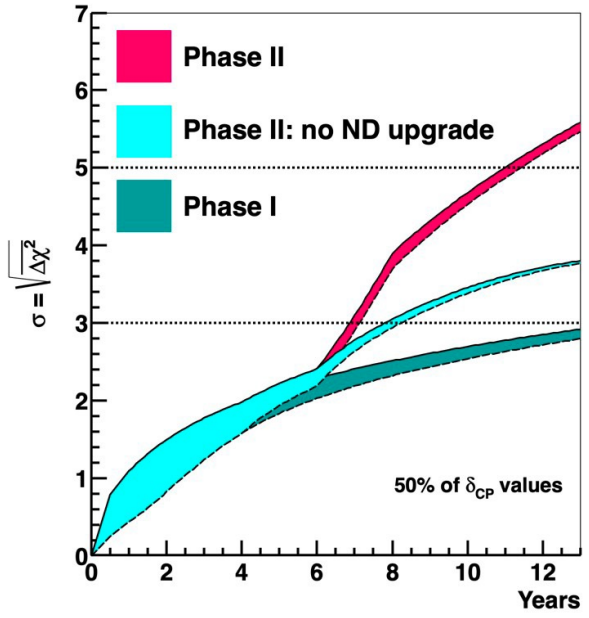

- To achieve the precision physics goals, including CPV sensitivity for a broad range of δCP values, all three upgrades are required
- Plots show the effect of removing one of them, resulting in a significant loss of sensitivity

Summary

- DUNE Phase I (start operation in 2029):
  - Two modules (HD/VD)
  - Beam (1.2 MW) in 2030
  - Near Detector (SAND, TMS+NDLAr, PRISM) in 2031
- DUNE Phase II (needed to reach physics goals)
  - Modules 3 and 4 (ongoing R&D)
  - Beam upgraded to 2.4 MW
  - Upgrade to Near Detector (ND-GAr)